*Russian Geology and Geophysics* © 2020, V.S. Sobolev IGM, Siberian Branch of the RAS
*Vol. 61, No. 3, pp. 303–321, 2020* *DOI:10.15372/RGG2019081* *Geologiya i Geofizika*

# Geochemistry of Carbonates in Small Lakes of Southern West Siberia Exampled from the Holocene Sediments of Lake Itkul'

**A.E. Maltsev[a, ✉], G.A. Leonova[a], V.A. Bobrov[a], S.K. Krivonogov[a,b], L.V. Miroshnichenko[a], Yu.S. Vossel[a], M.S. Melgunov[a]**

[a] *V.S. Sobolev Institute of Geology and Mineralogy, Siberian Branch of the Russian Academy of Sciences, pr. Akademika Koptyuga 3, Novosibirsk, 630090, Russia*

[b] *Novosibirsk State University, ul. Pirogova 1, Novosibirsk, 630090, Russia*

Received 31 July 2018; received in revised form 12 November 2018; accepted 5 February 2019

**Abstract**—A 1.8 m thick core of the Holocene (7.9 $^{14}$C kyr BP) sediments of Lake Itkul' (Novosibirsk Region) has been studied. Based on the geochemical and lithostratigraphic properties of the bottom sediments, we have established the following stages of the lake evolution: (1) the beginning of sedimentation, 7.8–7.0 $^{14}$C kyr BP; (2) extreme shallowing with a probable complete drying, ~7.0–5.5 $^{14}$C ky BP; (3) rise in the water level, ~5.5–4.3 $^{14}$C kyr BP; (4) repeated shallowing, 4.3–2.8 $^{14}$C kyr BP; and (5) subsequent watering, 2.8–0 $^{14}$C kyr BP. At present, the lake again tends to shallowing. We have established that Lake Itkul' has mineral sediments with a high content of carbonates (up to 64%). The high concentrations of $HCO_3^-$ and $Ca^{2+}$ and stable saturation ($S/St > 1$) of the surface water cause a shift of the carbonate–calcium equilibrium toward the carbonate formation. The studied authigenic carbonates are aragonite and fine-grained aggregates of poorly crystallized calcite particles with different Mg contents. Aragonite is both biogenic (mollusk and ostracode shells) and chemogenic (formed during the lake shallowing). In addition to carbonates, the lacustrine sediments contain mixed-layer aluminosilicates, feldspars, and quartz. The presence of pyrite throughout the sediment section indicates reducing conditions and the activity of sulfate-reducing microorganisms. Carbonates (especially aragonite) are significantly enriched in strontium. Manganese does not form its own minerals but is present as an isomorphic impurity in authigenic carbonates.

*Keywords:* carbonate sediments, calcite, aragonite, authigenic minerals, forms of occurrence and geochemistry of Ca, Sr, and Mn, diagenesis

## INTRODUCTION

Carbonates play a crucial role in the chemical composition of the ocean and atmosphere. They perfectly record the facies depositional environments and the composition of provenance rocks owing to diverse isomorphism of the crystal lattice (Reeder, 1983). The presence of carbonates of different types in lacustrine bottom sediments reflects the varying physicochemical factors of sedimentation (throughout the lake evolution), such as the Mg/Ca ratio, water salt content, pH, carbonate alkalinity, and paleobasin bioproductivity, which, in turn, are controlled by the climate, topography, lake basin structure, and intrabasin conditions (Last, 2002; Solotchina, 2009).

In arid environments, carbonates primarily precipitate as highly magnesian calcite (and, sometimes, aragonite), and in humid environments, mostly as lowly magnesian calcite (Kholodov, 2006; Yudovich and Ketris, 2011). The composition and content of carbonate minerals can serve as good indicators of the regime of precipitation and lake water level fluctuations. Small, highly mineralized lakes are sensitive to climate changes, which makes them a convenient object for study of the geochemistry of carbonate sediments and the sediment genesis environments (Solotchina et al., 2008; Sklyarov et al., 2010).

In contrast to terrigenous sediments, carbonate deposits undergo repeated (secondary) transformations during lithogenesis owing to their high solubility; as a result, their structure changes. Dissolution of primary carbonates and subsequent migration, removal, or concentration of their mobile impurity elements (Mg, Sr, Fe, and Mn) are major factors governing the geochemical composition of carbonate deposits (Yudovich and Ketris, 2011). Carbonates are one of major geochemical barriers for dissolved $Sr^{2+}$ and $Mn^{2+}$ (as well as $Ca^{2+}$) during lithogenesis (Perel'man, 1989).

The main goal of our research was to study the geochemical composition of the carbonate–mineral sediments of small Lake Itkul' (southern West Siberia, Novosibirsk Region) and the distribution of chemical elements (Al, Fe, Na, K, Mg, Ca, Sr, Mn, Cu, Zn, etc.) in them. During sediment genesis, the geochemical behavior of Ca, Sr, and Mn in highly calcareous sediments is determined by the rate of precipitation of carbonates, which are a geochemical barrier

✉ Corresponding author.
*E-mail address:* maltsev@igm.nsc.ru (A.E. Maltsev)

for these elements. Study of the distribution of carbonates throughout the Holocene section of the lacustrine bottom sediments and of variations in their Mg contents will help to reconstruct the main stages of the lake evolution.

## THE OBJECT OF STUDY

The object of study is located in the forest–steppe zone of the Novosibirsk Region (Chulym district), within the East Baraba lowland (Fig. 1). There is a network of small rivers in this area, the Chulym River being the largest. Lake Itkul' lies 2.5 km from the Chulym, beyond its valley, and is separated from it by a linear hill (low ridge). The lake is not hydrologically connected to the river, as it lies at an absolute height of 141 m above sea level, whereas the river water line is at an absolute height of 136 m. There is an earlier active rill of excess-water runoff into the Chulym in the western part of the lake, with a float along it. Lake Itkul' is located at the eastern edge of the area of an aeolian low ridge, in a lowland with Lake Chany at the center. The low-ridge strata are a bed of Late Glacial loess-like loams overlying all relief elements, except for river floodplains (Volkov et al., 1969). These deposits are exposed along the Itkul' shores and are the main supplier of lacustrine sediments. In the north and south, the lake shores have an abrasion scarp formed in the loess-like loams of adjacent low ridges as a result of the wave activity. A geological survey (Organomineral..., 1990) showed that the low-ridge strata are formed by sand-silty clays. These deposits are calcareous and contain 10–15% calcite. The heavy fraction (2–3%) is composed of epidote, magnetite, titanomagnetite, goethite, and occasional zircon, garnet, and rutile. The sand-silty clays are saline.

Hollow Lake Itkul' lies in the depression between low ridges and has a shallow bay in the west (Fig. 1). The lake without a bay is 5.2 km in length (with a bay, 8.7 km), the maximum width is 3.7 km, the average depths in its central part are ~1.5–1.8 m (the maximum depth is 3 m), the water area is 15.1 km$^2$, and the drainage area is 124 km$^2$. Itkul' is a lake with a small watershed (the drainage factor is 8.2). The lake is fed with spring water and precipitation (Organomineral..., 1990) and is characterized by border overgrowing. The border is formed by a reed (*Phragmites communis* Trin.) belt with spots of communities of sago pondweed (*Potamogeton pectinatus* L.) and clasping-leaved pondweed (*P. perfoliatus* L.) along it. A weed bed occupies no more than 10% of the total water area of the lake (Zarubina, 2013).

## METHODS

**Sampling and preparation of water and bottom sediment samples.** The lake water was sampled with a bathometer, and its pH, Eh, and temperature were measured immediately. Water for trace-element analysis was sampled into plastic containers and preserved by addition of concentrated nitric acid, following the recommended technique (Abakumov, 1983). Water for hydrochemical analysis (cations and anions) was not preserved.

Two boreholes were drilled by the vibration method to depths of 1.8 and 1.9 m in the central part of the lake

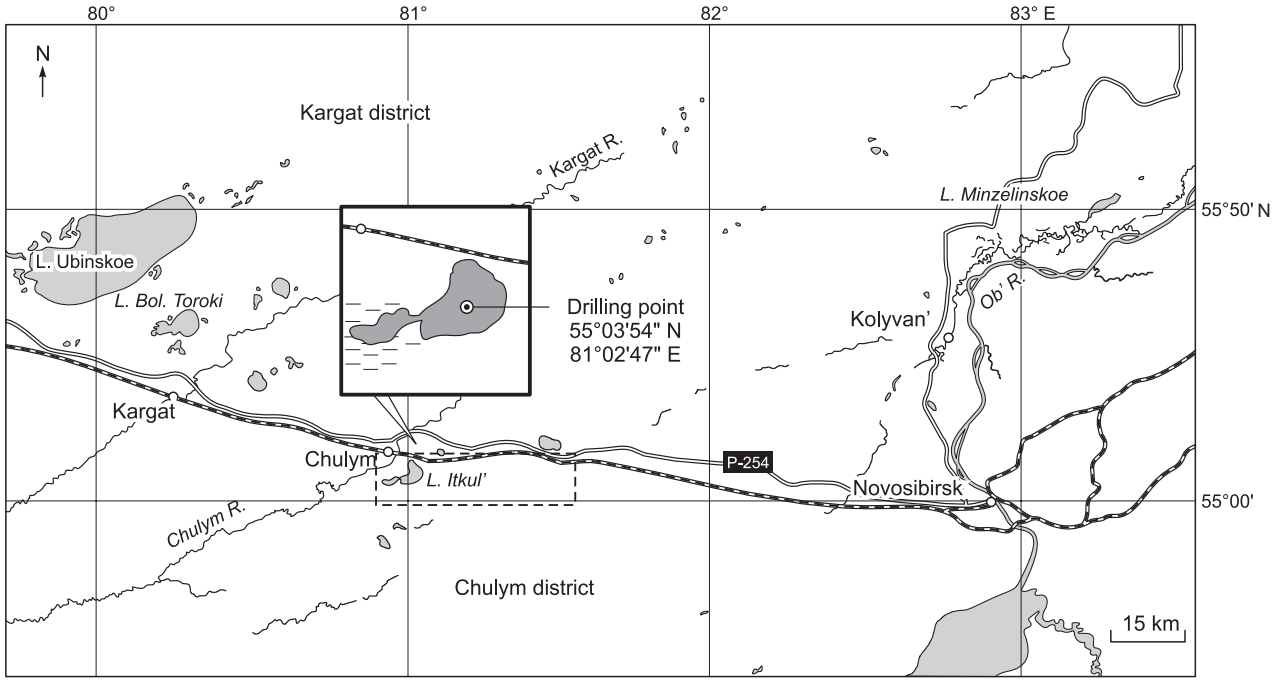


**Fig. 1.** Schematic map of the study area (Lake Itkul', Novosibirsk Region, Chulym district). Inset shows Lake Itkul' on a 1:200,000 scale map, with the drilling point and borehole coordinates.

(55°03′54″N, 81°02′47″E), using a Livingstone piston sampler. The penetrated lacustrine sediments are ~1.6 m thick and are underlain by low-ridge rocks. The drilling rig consisted of a pneumatic pontoon with a displacement of ~5 tons, a derrick with load-lifting mechanisms, and a pole drill 30 m in total length. The applied vibration drilling technology made it possible to penetrate the entire sediment strata and enter the underlying rocks. We obtained continuous undisturbed cores of the lacustrine sediments, 7.5 cm in diameter and 1.8–1.9 m in length. The cores were removed from the sampler, and their pH and Eh were measured. Then the undisturbed cores were hermetically sealed in polyethylene and plastic cases and transported to the laboratory, where they were described and sampled at 2–5 cm intervals for different analyses.

**Analytical methods.** Hydrochemical analysis (determination of the contents of $K^+$, $Na^+$, $Ca^{2+}$, $HCO_3^-$, $Cl^-$, $SO_4^{2-}$, $NO_3^-$, $NO_2^-$, and $PO_4^{3-}$) of the Itkul' water was carried out in the Laboratory for Control of Natural and Waste Water Quality of the VerkhneOb'regionvodkhoz Federal State Institution (analysts T.M. Bulycheva and G.N. Krivopalova), following generally accepted techniques (Technique..., 2004, 2005; Mass Concentration..., 2006).

The bulk contents of Hg, Pb, Cd, Cu, Zn, Ni, Cr, Co, Fe, and As in solid and water samples were determined by atomic-absorption spectrometry (AAS) at the Analytical Center for Multi-Elemental and Isotope Research of V.S. Sobolev Institute of Geology and Mineralogy, Novosibirsk (analysts V.N. Il'ina and N.V. Androsova). Analyses for Zn, Fe, and Mn were carried out by flame AAS. The contents of Hg were determined by the "cold steam" method with amalgamation of the element on a gold sorbent (analyst Zh.O. Badmaeva). The contents of Al, B, Ba, Ca, Mg, Sr, P, Na, K, Li, Cr, Ni, Co, Mo, Fe, Mn, Cu, Zn, As, Sb, and Ti in water and bottom sediments were measured by ICP-AES (analyst S.F. Nechepurenko). Analyses for REE in the bottom sediment samples were performed by ICP-MS (chemical sample preparation by I.V. Nikolaeva; instrumental measurements by S.V. Palesskii). The contents of major rock-forming oxides were determined by X-ray fluorescence analysis (analyst N.G. Karmanova). The mineral composition of the sediments was studied by XRD, using a DRON-4 diffractometer with $CuK_\alpha$ radiation (analyst L.V. Miroshnichenko).

The radioactivity of the upper beds of the sediment was measured by semiconductor gamma spectrometry in the Laboratory of Geochemistry of Noble and Rare Elements and Ecogeochemistry of the Institute of Geology and Mineralogy, Novosibirsk, using a low-background gamma spectrometer with a coaxial well-type HPGe detector (200 $cm^3$) with the following sensitivity to radionuclides: 0.05 Bq ($^{210}$Pb, $^{226}$Ra, $^{238}$U, and $^{137}$Cs), 0.01 Bq ($^{232}$Th), and 0.3 Bq ($^{40}$K) (analyst M.S. Mel'gunov).

The quantitative content of carbonates in the sediments was determined following the technique described by Vorob'eva (1998). The content of organic carbon ($C_{org}$) in the samples was evaluated by Tyurin's technique (Vorob'eva, 1998) at the Institute of Soil Science and Agrochemistry, Novosibirsk (analyst L.D. Cherepakhina). The micromorphology and chemical composition of the bottom sediments were studied using a TESCAN MIRA 3 LMU electron scanning microscope.

The forms of occurrence of chemical elements in the bottom sediments were determined by the selective-dissolution method (stepwise leaching) (Klemt et al., 2000). To identify Mn forms, we applied this method adapted for carbonate sediments. After leaching, the obtained solutions were analyzed for Ca, Mg, Mn, and Fe by AAS (analysts I.V. Makarova and L.D. Ivanova, V.S. Sobolev Institute of Geology and Mineralogy). Manganese oxides and hydroxides partly dissolve during this analysis of carbonates (Fedotov and Spivakov, 2008); therefore, we additionally used electron paramagnetic resonance (EPR) permitting separation of Mn of carbonates from Mn of oxide phases. The EPR spectra of the samples were recorded on a Brukker spectrometer with a double resonator at Voevodsky Institute of Chemical Kinetics and Combustion, Novosibirsk (analyst D.V. Stas'). The EPR spectra look like a typical spectrum of $Mn^{2+}$ in calcite. They show six hyperfine doublets spaced ~94 Gs apart, with pairs of forbidden transitions between them. The content of $Mn^{2+}$ in the sample calcites was determined from the integrated spectrum intensity, which was measured by double integration of the low-field hyperfine doublet and was compared with the integrated intensity of the standard sample. The content of $Mn^{2+}$ in the latter measured by AAS is 80 mg/kg.

**Determination of the accumulation of chemical elements in the bottom sediments.** Organic, organomineral, and mineral bottom sediments can accumulate chemical elements to different degrees. The degree of element accumulation can be expressed as an enrichment factor (*EF*), i.e., the ratio of the content of the *i*-th element under study to the content of a certain reference element (Sc, Al, Cr, or Ti). The *EF* value was calculated by the technique of Shotyk et al. (1966), by normalization of the contents of all chemical elements in the bottom sediments to the content of Al, a reference element (Lukashin, 1981; Monin and Lisitsyn, 1983). To determine the geochemical specifics of the objects under study, we used argillaceous shales with a permanent chemical composition (Li, 1991), typical of continental water reservoirs, as a reference sample. The *EF* value for the bottom sediments was calculated by the formula (Shotyk et al., 1966).

$$EF = (x_i/x_{Sc})_{samp}/(x_i/x_{Sc})_{arg.\ shale},$$

where $x_{i\ samp}$ is the content of the *i*-th chemical element in the object under study, $x_{Sc\ samp}$ is the content of Sc in it, $x_{i\ arg.\ shale}$ is the content of the *i*-th chemical element in argillaceous shale, and $x_{Sc\ arg.\ shale}$ is the content of Sc in it.

**Calculation of geochemical parameters.** We estimated the contribution of terrigenous and authigenic calcium ($Ca_{terr}$ and $Ca_{auth}$, %) to the Lake Itkul' sediments, taking Al as a reference element (the contents of Al and Ca in the upper

continental crust are 7.74% and 2.94%, respectively (Wedepohl, 1995)), as follows:

$$Ca_{terr} = (Al_{samp}/Al_{cr}) \times Ca_{cr}, \quad (1)$$

where $Al_{samp}$ is the content of Al in the certain lacustrine-sediment horizon, $Al_{cr}$ is the content of Al in the upper continental crust, and $Ca_{cr}$ is the content of Ca in the upper continental crust (Wedepohl, 1995),

$$Ca_{auth} = Ca_{tot} - Ca_{terr}, \quad (2)$$

where $Ca_{tot}$ is the total content of Ca in the certain lacustrine-sediment horizon, $Ca_{terr}$ is the content of terrigenous Ca calculated by (1), and $Ca_{auth}$ is the content of authigenic Ca (chemogenic and biogenic).

The coefficient of Ca migration in water ($K_x$) was calculated by the formula (Perel'man, 1982)

$$K_x = m_x \times 100/a \times n_x,$$

where $m_x$ is the content of Ca in water, g/L, $n_x$ is the content of Ca in the bottom sediments, wt.%, and $a$ is the water salinity, g/L.

To evaluate the saturation of the Itkul' surface water with $CaCO_3$, we used the ratio of the ion activity product $S = \alpha Ca^{2+} \times \alpha CO_3^{2-}$ in the water to the experimental ion activity product for $CaCO_3$ ($St$) (Alekin and Moricheva, 1962):

$$S/St = [Ca^{2+}] \times [CO_3^{2-}] \times (f'')^2 / S_{CaCO_3(t°)},$$

where $S_{CaCO_3(t°)}$ is the ion activity product for $CaCO_3$ at 20 °C (sampling temperature) (Alekin and Moricheva, 1962), $f''$ is the activity coefficient at the ionic strength of the solution (μ) equal to 0.005, and the ion concentrations are given in mol/L.

Water with $S/St < 0$ is not saturated with $CaCO_3$, water with $S/St > 1$ is oversaturated with $CaCO_3$, and water with $S/St = 1$ is normally saturated with $CaCO_3$.

**Table 1.** Major hydrogeochemical indices of the Itkul' surface water

| Index | Value |
|---|---|
| $T$, °C | 19.6 |
| pH | 9.1 |
| Transparency, cm | 30 |
| Eh, V | +0.167 |
| TH, mg-eq/L | 9.44 |
| $O_2$, mg/L | 6.5 |
| CCO, mg$O_2$/L | 126.4 |
| BCO, mg$O_2$/L | 3.7 |
| $C_{org}$, mg/L | 47.4 |
| $HCO_3^-$, mg/L | 1220.0 |
| $SO_4^{2-}$, mg/L | 36.0 |
| $Cl^-$, mg/L | 365.8 |
| $NO_3^-$, mg/L | 1.1 |
| $NO_2^-$, mg/L | 0.062 |
| $PO_4^{3-}$, mg/L | 0.028 |
| $Ca^{2+}$, mg/L | 24.0 |
| $Mg^{2+}$, mg/L | 100.1 |
| $Na^+$, mg/L | 333.3 |
| $K^+$, mg/L | 17.1 |
| $NH_4^+$, mg/L | 0.41 |
| TDS, mg/L | 2098 |
| $K_x$ | 0.1 |
| $S/St$ | 2.25 |

Note. TH, total hardness of water; CCO, chemical consumption of oxygen; BCO, biologic consumption of oxygen; TDS, total dissolved salts; $K_x$, coefficient of Ca migration in water; $S/St$, ratio of the activity product of $Ca^{2+}$ and $HCO_3^-$ to the thermodynamic $CaCO_3$ solubility product at 20 °C. Hydrochemical analysis of water was determined in the Laboratory of Control of Natural and Waste Water Quality of the VerkhneOb'regionvodkhoz Federal State Institution (analysts T.M. Bulycheva and G.N. Krivopalova).

## THE CHEMICAL COMPOSITION OF THE LAKE WATER AND THE CARBONATE–CALCIUM EQUILIBRIUM

The Itkul' surface water is predominantly of sodium hydrocarbonate composition (Alekin, 1970). It is oxidized (Eh = +0.167 V), oxygen-enriched ($O_2$ (dissolved) = 6.5 mg/L), highly alkaline (pH = 9.1) brackish (TDS = 2098 mg/L) water (Perel'man, 1989). Its main ionic composition is given in Table 1. The surface water has high concentrations of $Cl^-$, $SO_4^{2-}$, $Na^+$, and $Mg^{2+}$. Ions $Cl^-$, $Na^+$, and $Mg^{2+}$ might have been supplied to the water from the drainage soils with obvious signs of solodization and alkalinity (Syso, 2007). The inverse proportion of sulfate and calcium ions ($SO_4^{2-} > Ca^{2+}$) in the lake surface water (Table 1) indicates its metamorphization, with the replacement of $Ca^{2+}$ by $Na^+$ and $Mg^{2+}$, which is specific to mineralized water. The limited solubility of $CaCO_3$ (ensuring continuous removal of $CaCO_3$ from the aqueous solution) determines low concentrations of $Ca^{2+}$ relative to $Na^+$ and $Mg^{2+}$. The accumulation of $HCO_3^-$, $Na^+$, and $Cl^-$ in the lake is due to the metamorphization of its surface water by the evaporative-concentration mechanism, i.e., the concentrations of $Cl^-$ and the pH values increase with the content of carbonates (Shvartsev, 1998; Zamana, 2009).

In addition to major ions, we detected macroelements (Si, Al, P, and Fe) and trace elements (Ti, V, Cr, Mn, Co, Ni, Cu, Zn, Rb, Sr, Mo, Cd, Hg, and Pb) in the Itkul' water, which determine the hydrogeochemical specifics of the limnological geosystem of the lake. Its surface water is characterized by high concentrations of Si (5700 μg/L), Al (405 μg/L), and Sr (500 μg/L) and elevated concentrations of Ti (7.2 μg/L) and U (1.2 μg/L) (Table 2).

Lake Itkul' has favorable conditions for the precipitation of $CaCO_3$: Its basin has an intricate structure, with vast open shallow-water zones prevailing over smaller deep zones. At shallow depths without water stratification, the carbonate formation zone covers the entire water layer of the lake.

**Table 2.** Elemental composition of the Itkul' surface water

| Element | μg/L | Element | μg/L | Element | μg/L | Element | μg/L |
|---|---|---|---|---|---|---|---|
| Si | 5700 | Cu | 2.6 | Ag | 0.01 | Eu | 0.0300 |
| Al | 405 | Zn | 10 | Cd | 0.041 | Gd | 0.080 |
| P | 58 | U | 1.2 | Sb | 0.14 | Tb | 0.0100 |
| Ti | 7.2 | Rb | 3.4 | Cs | 0.02 | Dy | 0.050 |
| V | 12 | Sr | 500 | Ba | 75 | W | 0.01 |
| Cr | 2.3 | Y | 0.40 | La | 0.36 | Pt | 0.02 |
| Mn | 38 | Zr | 0.39 | Ce | 0.63 | Hg | <0.010 |
| Fe | 518 | Nb | 0.02 | Pr | 0.09 | Pb | 0.85 |
| Co | 0.8 | Mo | 1.5 | Nd | 0.320 | Th | 0.01 |
| Ni | <1 | Pd | 0.04 | Sm | 0.06 | | |

Note. The bulk concentrations of chemical elements were determined by AAS (analysts V.N. Il'ina, N.V. Androsova, and Zh.O. Badmaeva) and ICP MS (analysts S.V. Palesskii and I.V. Nikolaeva) at the Analytical Center for Multi-Elemental and Isotope Research of V.S. Sobolev Institute of Geology and Mineralogy.

Table 1 presents major indices of the carbonate–calcium equilibrium in the lake water. The water is characterized by stable saturation conditions, $S/St > 1$ (on the background of high pH values), and the calcium–carbonate equilibrium is shifted to the precipitation of carbonates. Calcium is poorly mobile in the lake water ($K_x = 0.1$), which is atypical of calcium in the surface hydrocarbonate water of most of freshwater lakes ($K_x = 1–10$ (Perel'man, 1982)). The poor migration of Ca in the brackish water of Lake Itkul' (TDS = 2 g/L) is due to its active removal in the form of authigenic carbonates. The current high concentrations of $Mg^{2+}$ in the lake water (0.1 g/L) favor the prevailing chemogenic precipitation of Mg–$CaCO_3$ (with different contents of Mg).

## THE STRUCTURE AND AGE OF THE SEDIMENTS AND THE SEDIMENTATION RATES

The Itkul' sediments are ~1.6 m thick carbonatized mineral muds of homogeneous composition (Fig. 2). They consist mostly of pelite and silt fractions and virtually lack a sand fraction. Apparently, sand present in a minor amount in the eroded loess strata does not reach the central zone of the lake. The sediment column is formed by beds of different colors: depth range 0–55 cm—light gray, 55–106 cm—dark gray, 106–138 cm—gray (with the range 136–138 cm being somewhat lighter), and 138–162 cm—dark gray. The lacustrine sediments occur to a depth of 162 cm. In the range 136–138 cm, black dissemination 0.5–1.0 mm in size, ostracode shells, and rare plant and seed remains are found. In the range 145–160 cm, there are a small number of fragments of bivalve and snail shells and of ostracodes. Below a depth of 162 cm, there are the underlying loess-like sediments of a low ridge.

Sedimentological analyses (Fig. 2) show significant differences in the composition and properties of the loesses and lacustrine sediments. The lake beds are subdivided into 2–4 depth ranges. In the depth range 60–55 cm, the average water content of the sediments drastically changes from 50 to 60% because of a stepwise change in the average density of the sediments from 0.71 to 0.53 g/cm$^3$. The changes in the sediment composition are reflected in the negative correlation between the contents of the authigenic and terrigenous fractions. In the depth range 165–145 cm, there are the maximum content of the terrigenous fraction (~90%) and the minimum content of the authigenic fraction (~10%). In the depth range 145–125 cm, there are the maximum content of the authigenic fraction (up to 80%) and the minimum content of the terrigenous fraction (up to 10%). Upsection, the content of the terrigenous fraction shows a stepwise increase and the content of authigenic fraction decreases. Stable conditions are observed in the depth ranges 120–105, 100–80, and 70–10 cm. The surface sample has a lower portion of the terrigenous fraction and a higher portion of the authigenic fraction, which reflects the current state of the lake. The ash content in the sediments is within 86–96%, drastically decreasing to 85.6% at a depth of 136 cm. This is the only change that shows correlation with the changes in the contents of other sediment fractions. In the rest of the section, there are four rhythms of changes in the ash content, which probably reflect changes in the intensity of the inflow of terrigenous material into the lake but are poorly correlated with changes in the contents of other sediment components. An increase in the ash content in the middle depth ranges (80–130 cm) on the background of the decreasing content of $SiO_2$ and increasing content of CaO indicates a greater contribution of carbonates to the total ash content in this sediment zone (Fig. 2).

The above data on changes in the composition and properties of the sediments obviously reflect changes in the depositional environments and can be interpreted as fluctuations in the lake water level and as changes in the lake salinity. Figure 3*a* shows a rough coincidence of the visual boundaries and the boundaries of changes in the sediment composition. The data on the ratio of terrigenous (T) and authigenic

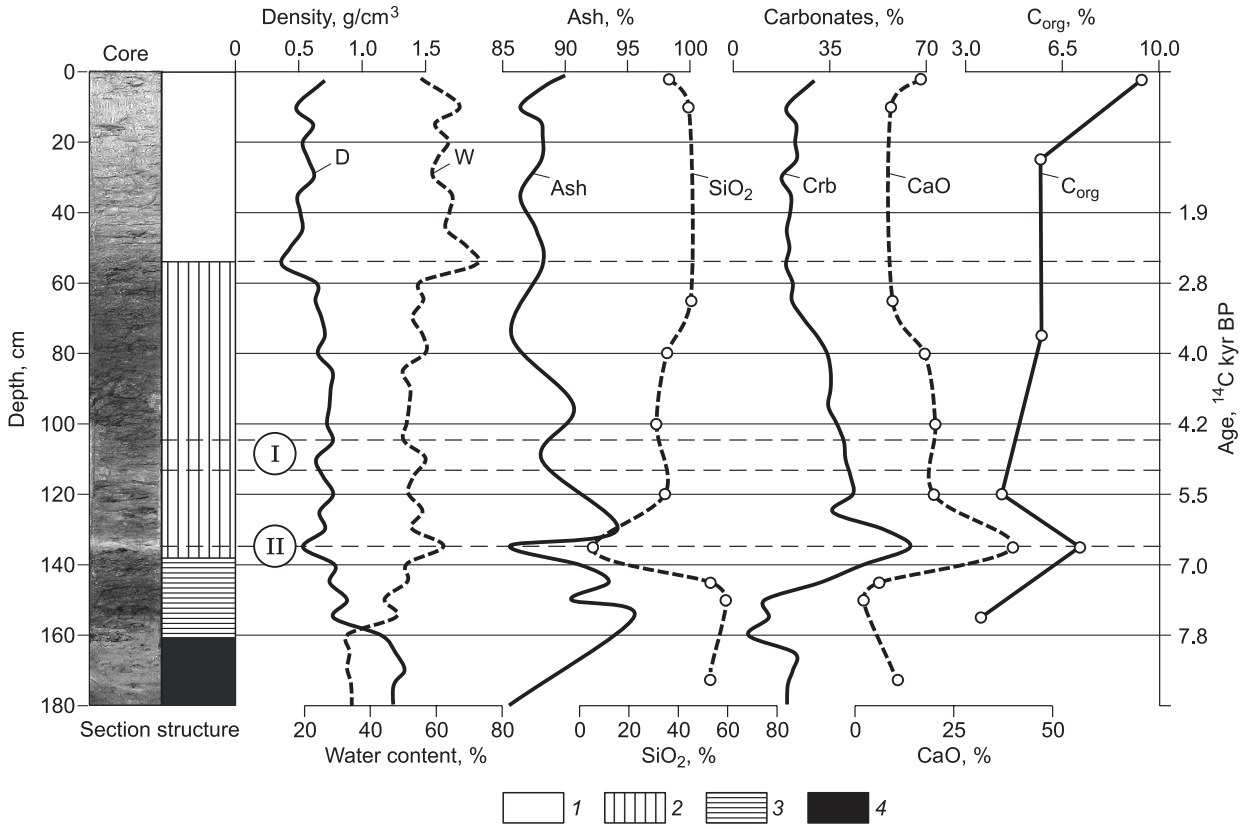


**Fig. 2.** Structure of the Itkul' lacustrine sediments, their age, and vertical distribution profiles of density (D), water content (W), ash content (Ash), and contents of $SiO_2$, carbonates (Crb), CaO, and $C_{org}$. *1*, 0–55 cm, light gray loam (lacustrine mud), humid, with rare plant remains; *2*, 55–138 cm, more compact dark gray loam, including darker clay with a sandy material (range 55–100 cm), a less compact bed (I) (107–114 cm), and a small light brown interbed (II) (136–138 cm); *3*, 138–162 cm, dark brown argillaceous material with fragments of mollusk shells; *4*, 162–180 cm, underlying dark gray (bluish) loess-like loams. The ash content was determined at 450 °C; the $^{14}C$ age of the sediments was determined by accelerator mass spectrometry. The contents of the sediment components were calculated on anhydrous basis.

(A) fractions of the sediments are the most informative. If we interpret the increase in the portion of the terrigenous fraction as shore erosion and the increase in the portion of the authigenic fraction as an increase in water salinity, then we obtain the following sequence. At the initial stage (depth range 162–145 cm), a rather large freshwater lake appeared, which actively washed out its shores. Then, the water level drastically fell, and the water became saline (145–125 cm). Later, the water level rose step by step, and the lake gradually became fresh (125–10 cm). The subsurface sedimentary bed (10–0 cm) reflects a tendency toward a current decrease in water level and water salinization.

Accelerator mass spectrometry (AMS) radiocarbon dating (Table 3) showed that the bottom sediment strata formed in the middle Holocene over 7.8 $^{14}C$ kyr BP (8.8 cal kyr BP). The obtained dates, except for the date estimated at a depth of 20 cm, form a stratigraphically consistent sequence. Therefore, the date estimated at a depth of 20 cm was ignored. The age model (Fig. 3*b*) shows a linear trend reflecting more or less regular sedimentation with an average rate of 0.18 mm/yr. The trend deviates by ~200 yr toward rejuvenation at the point 0 $^{14}C$ yr (1950 AD). The use of a polynomial trend eliminates this drawback. Both trends are characterized by high confidence $R^2$.

The ages of the stratigraphic and geochemical boundaries were calculated from $^{14}C$ dates. To reduce the error of calculation of these ages, we used the point 0 $^{14}C$ yr and linear interpolation between the dates. Applying linear interpolation reduces the probable error of dating at distance from the points of the measured ages.

## MINERALOGICAL AND GEOCHEMICAL CHARACTERISTICS OF THE SEDIMENTS

**$C_{org}$, Eh, and pH.** Figure 2 shows the distribution of organic carbon ($C_{org}$) throughout the section of the Itkul' bottom sediments. The content of $C_{org}$ is low (on average, 6%) and varies from 3.6% near the base to 9.3% near the roof of the section. In the depth range 136–138 cm, the content of $C_{org}$ increases from 3.6 to 7.1%. The presence of even a small amount of organic matter (OM) in the sediments ensures reducing conditions in the upper depth ranges (0–2 cm), with Eh = –171 mV. With depth, the Eh values

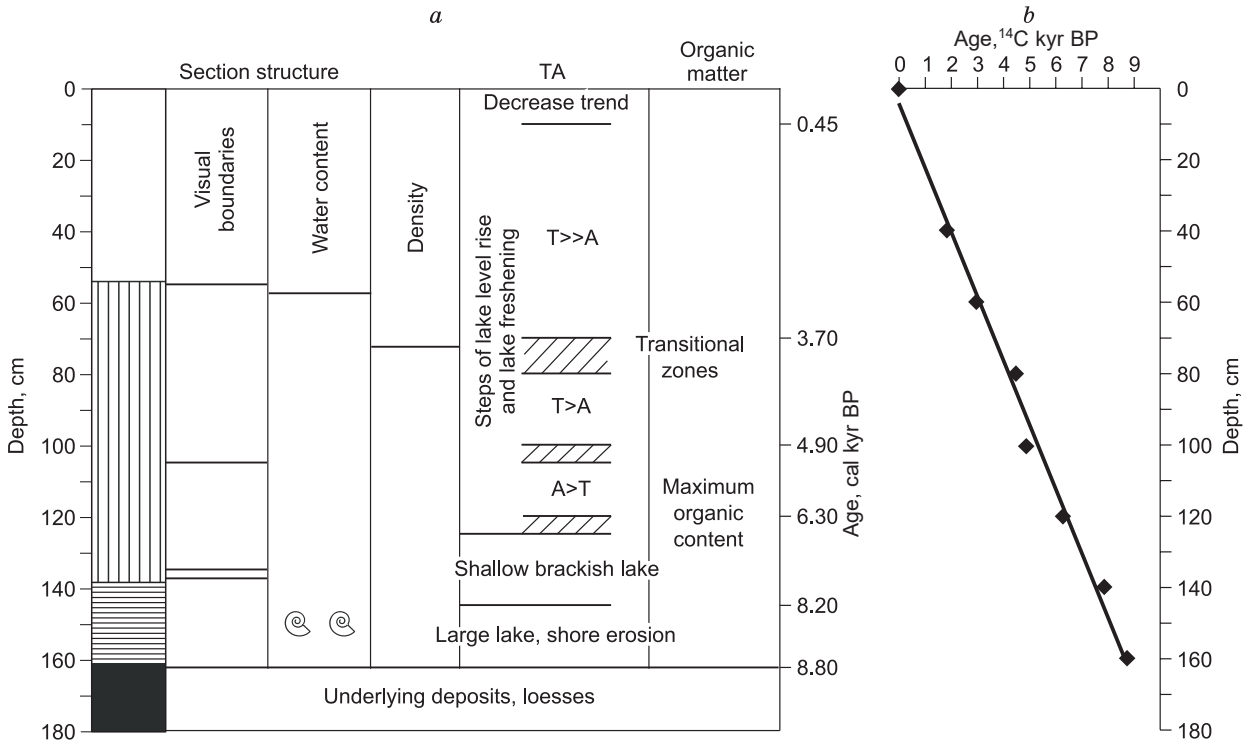


**Fig. 3.** Changes in the depositional environment (*a*) and age model (*b*) of Lake Itkul'. T, terrigenous fraction of the sediments; A, authigenic fraction of the sediments. Designations follow Fig. 2.

drastically decrease (–329 mV, 100 cm), reaching –377 mV at a depth of 180 cm. Thus, Lake Itkul' lacks an oxidized sedimentary bed, and all geochemical processes in the bottom sediments run under anaerobic conditions. The pH values in the upper intervals of the sediments are lower as compared with the lake water (8.2 against 9.1). Apparently, the pH decrease is related to the destruction of OM resulting in $CO_2$ and organic acids, which leads to acidification of the medium.

**Chemical composition.** The major component of the Itkul' bottom sediments is $SiO_2$, whose average content in the section is 39.7% (Table 4). The average contents of CaO and $Al_2O_3$ are 15.1 and 9.5%, respectively. According to the prevailing components of their mineral part (CaO and $SiO_2$), the Itkul' sediments are of mixed carbonate-siliceous type. Following the classification by Lukashev et al. (1971), they are marly clay. The lower depth range of the lacustrine sediments (145–152 cm) is richer in $SiO_2$ and $Al_2O_3$ than the overlying interval (0–136 cm). In the middle depth range (122–80 cm), the contents of $SiO_2$ and $Al_2O_3$ are slightly lower, and the portion of CaO increases to 17.7–20.3% as compared with the upper range (10–66 cm). The highest CaO content (40%) is found in the narrow horizon 136–138 cm. According to the contents of CaO and $SiO_2$, the

**Table 3.** Results of radiocarbon dating and calibration of dates estimated for the Itkul' sediments from the content of dispersed organic matter (TOC)

| Depth, cm | $^{14}C$ age, kyr BP | Range of calibrated ages, kyr BP | Median value of the most probable age, kyr BP |
|---|---|---|---|
| 20 | 2005 ± 153 | – | – |
| 40 | 1873 ± 120 | 1542–2112 | 1808 |
| 60 | 2821 ± 136 | 2724–3345 | 2966 |
| 80 | 3985 ± 132 | 4092–4830 | 4456 |
| 100 | 4292 ± 140 | 4451–5299 | 4874 |
| 120 | 5486 ± 171 | 5914–6651 | 6270 |
| 140 | 7001 ± 170 | 7524–8174 | 7835 |
| 160 | 7829 ± 315 | 8044–9436 | 8718 |

Note. AMS radiocarbon dating was carried out by A.V. Petrozhitskii and E.V. Parkhomchuk at the Cenozoic Geochronology Common Use Center, Novosibirsk. Calibration was made using the Calib $^{14}C$ software (version 7.10): http://calib.org/calib/calib.html.

sediments in this range are lake lime. Below a depth of 138 cm, the CaO content decreases to 10% (Fig. 2), and the content of MgO, to 1.9%.

**Mineral composition.** According to XRD data, the main minerals in the Itkul' bottom sediments are plagioclase, calcite, aragonite, and quartz (Fig. 4). Pyrite, mica, K-feldspar (absent at a depth of 136 cm), kaolinite (absent from the underlying loam at a depth of 170 cm), amphiboles (absent at depths of 100 and 136 cm), and chlorite are ubiquitous in the section. Ilmenite $FeTiO_3$ was found in the upper horizons (0–10 cm) of the bottom sediments (Fig. 4*a*). Traces of gypsum are found at depths of 100 and 136 cm, which might be due to a change in the lake water salinity.

Calcites (Mg-$CaCO_3$ and $CaCO_3$) occur throughout the bottom sediment section. Magnesian calcite is found in the depth range 0–136 cm and disappears below a depth of 145 cm. Its total content in the section is much lower than the content of $CaCO_3$ (Fig. 4). An exception is the depth range 120–138 cm, where the content of Mg-$CaCO_3$ is higher than that of $CaCO_3$. The upper depth ranges (0–80 cm) are poor in Mg-$CaCO_3$. Aragonite is absent from most of the section; it occurs only in the depth range 80–100 cm and in

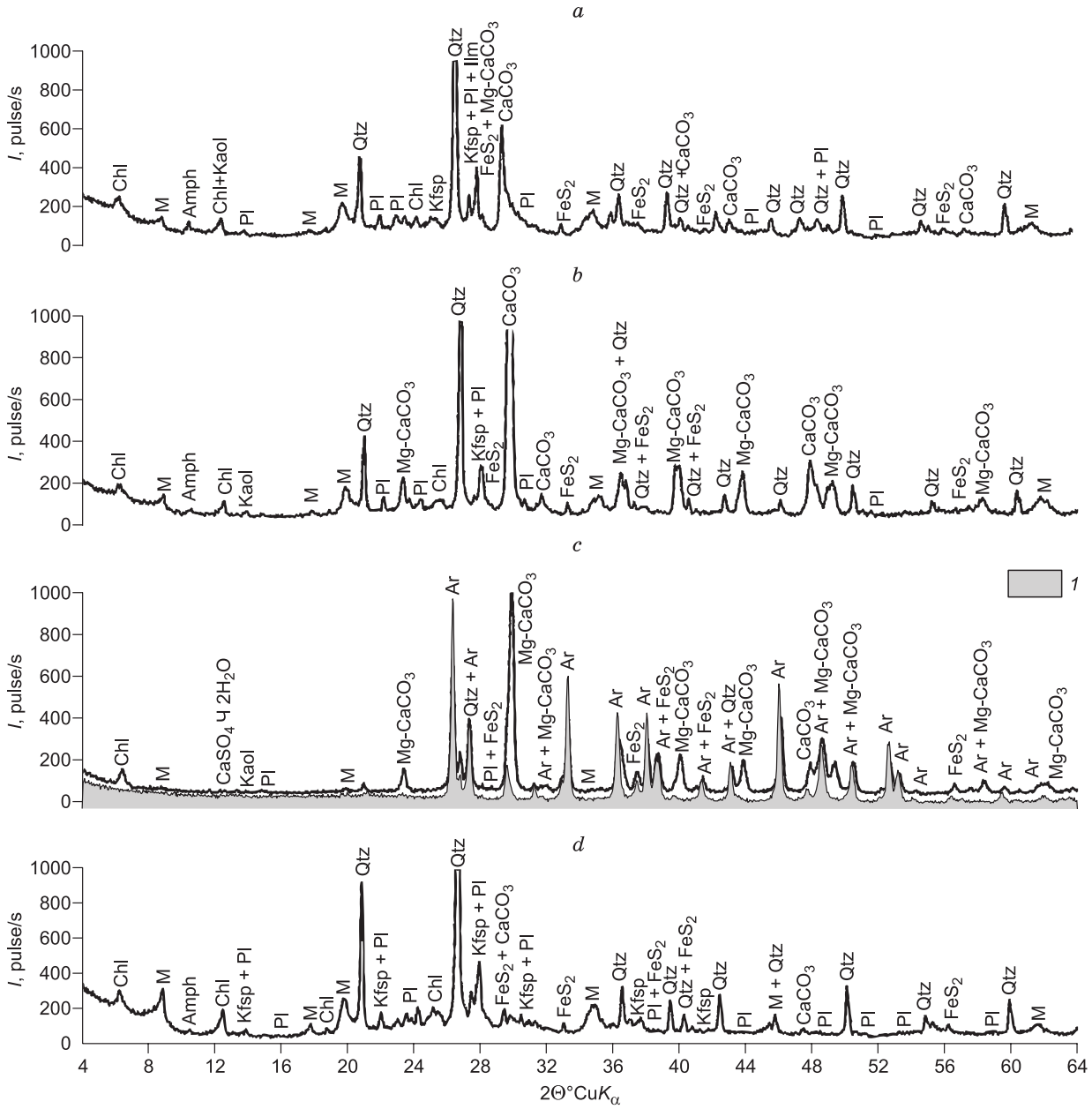


**Fig. 4.** XRD spectra of different depth ranges of the Itkul' bottom sediments: *a*, Argillaceous material with plant remains (10 cm); *b*, dark sandy clays with "humus" interbeds (120 cm); *c*, light clays (136 cm) and shells (*1*) (145–160 cm); *d*, sandy clays (150 cm). Minerals: Amph, amphibole; Ar, aragonite; Ilm, ilmenite; Kaol, kaolinite; Qtz, quartz; Kfsp, K-feldspar; Pl, plagioclase; M, mica; Chl, chlorite.

**Table 4.** Chemical composition of the Itkul' bottom sediments

| Horizon, cm | LOI | $SiO_2$ | $Al_2O_3$ | $Fe_2O_3$ | MgO | CaO | $Na_2O$ | $K_2O$ | $SO_3$ |
|---|---|---|---|---|---|---|---|---|---|
| | wt.% | | | | | | | | |
| 0–2 | 23.21 | 36.30 | 8.83 | 4.25 | 3.23 | 16.63 | 0.82 | 1.61 | 2.99 |
| 10–12 | 22.02 | 44.27 | 10.45 | 4.57 | 3.76 | 9.11 | 0.93 | 1.82 | 1.50 |
| 64–66 | 19.26 | 45.10 | 11.00 | 4.81 | 3.56 | 9.51 | 0.91 | 1.97 | 2.07 |
| 80–82 | 23.86 | 35.35 | 8.28 | 3.99 | 3.51 | 17.66 | 0.79 | 1.48 | 3.24 |
| 100–102 | 25.42 | 31.07 | 7.80 | 4.34 | 2.63 | 20.34 | 0.71 | 1.40 | 4.79 |
| 120–122 | 24.96 | 34.48 | 8.30 | 3.43 | 2.66 | 19.94 | 0.78 | 1.59 | 2.36 |
| 136–138 | 43.91 | 5.21 | 1.35 | 1.48 | 1.86 | 39.97 | 0.32 | 0.23 | 4.18 |
| 145–147 | 13.03 | 53.09 | 12.76 | 4.92 | 2.41 | 6.12 | 1.04 | 2.68 | 1.91 |
| 150–152 | 8.61 | 59.50 | 14.44 | 5.63 | 2.54 | 2.15 | 1.16 | 3.02 | 1.18 |
| 170–172 | 11.52 | 53.12 | 12.07 | 4.64 | 2.26 | 9.58 | 1.10 | 2.34 | 0.95 |
| Average over the section | 21.6±9.9 | 39.7±15 | 9.5±3.6 | 4.2±1.1 | 2.8±0.6 | 15.1±10 | 0.9±0.2 | 1.8±0.7 | 2.5±1.2 |

Note. Data are calculated on anhydrous basis. LOI, loss on ignition in air at 900 °C. Contents of major rock-forming oxides were determined by X-ray fluorescence analysis in the Laboratory of X-Ray Spectral Analytical Methods of V.S. Sobolev Institute of Geology and Mineralogy (analyst N.G. Karmanova).

the narrow horizon 136–138 cm, where its content is much higher than the contents of calcite and Mg-calcite (Fig. 4). In the depth range 145–150 cm, the content of calcite is minimum and Mg-calcite is absent. The content of calcite in the loess-like loams underlying the sediments is higher than its content in the sediment interval 145–150 cm. Magnesian calcite is absent from the underlying loams. Shells sampled from the depth range 145–160 cm are composed of predominant aragonite and minor Mg-calcite (Fig. 4*c*).

**Electron microscopy.** In the electron scanning microscope (SEM) images, carbonates are fine-grained aggregates of poorly crystallized particles of variably magnesian calcite (Fig. 5) as well as aragonite of Planorbidae and Ostracoda shells from the lower sediment intervals (Fig. 5*c*). Carbonates of the shells are slightly enriched in Sr (Fig. 5*e*) and, sometimes, Mg; there are also shells formed by carbonates without impurities. Sometimes, carbonates of the sediments are sheared $CaCO_3$ and Mg-$CaCO_3$ plates up to 100 μm in size and larger (Fig. 5*b*, *c*). These are probably shell fragments. Calcite from the middle depth range of the sediments (100–138 cm) contains an impurity of Mg (about 1–5 wt.%, according to SEM data). In argillaceous material from the upper depth range (0–10 cm), there are plant remains with surficial lamellar $CaCO_3$ aggregates containing impurities of Mg (~1 wt.%) and Mn (0.5–0.8 wt.%) (Fig. 5*f*).

According to the SEM data, the sediments are rich in quartz and also contain K-feldspar and plagioclase. Pyrite is present both as framboids and as individual crystals (Fig. 5*a*, *b*, *d*). The presence of pyrite in the sediments on the background of low Eh values indicates the high activity of sulfate-reducing microorganisms. Single barite crystals were found at depths of 60 and 136 cm (Fig. 5*c*). Rutile and ilmenite crystals measuring ~10 μm were found in the upper 2 cm horizon of the sediments. Ilmenite crystals up to 50 μm in size were also revealed at a depth of 150 cm (Fig. 5*a*, *d*). In the upper 0–2 cm range of the sediments, monazite crystals 5–7 μm in size were detected. Under bedrock destruction, monazite, a stable and mechanically strong mineral, passes into placers together with ilmenite, rutile, and other genetically related minerals (Kozlovskii, 1984).

**Distribution of chemical elements** in the Itkul' sediments is presented in Table 5 and in Fig. 6. The change in the chemical composition of the sediments throughout their section determines the distribution patterns of Al, K, Na, Mg, Fe, Ni, Li, Co, Ca, Sr, and Mn. For example, the contents of Al, K, Na, Mg, Fe, Ni, Li, and Co in the depth range 0–55 cm are high (Table 5), and in the range 55–114 cm they are slightly lower. The maximum contents of these elements are found in the underlying loess-like loams (162–180 cm). The content of Al slightly decreases (to 3.8%) in the transitional interval (138–162 cm). In the depth range 136–138 cm, the contents of the above elements are minimum, whereas the contents of Ca and Sr (and, in places, Mn) are extremely high. In general, the low contents of Al, Fe, K, Na, Zn, Ni, Cu, Pb, Cr, and Be and abnormally high contents of Ca and Sr in this interval are due to the "dilution" of the terrigenous component of the sediment by carbonates, which actively precipitated at this stage of the lake evolution. The distribution of Be, Cr, and V throughout the section matches the distribution of Al (Table 5). The distribution pattern of chalcophile elements (Cu, Zn, and Pb) is similar to those of lithophile elements (Al, K, Na, Ni, and Co) (but does not match the distribution patterns of As, Hg, and Cd). In the depth range 100–130 cm, the contents of Ca increase from 6–7 to 12–16%, i.e., twice (Table 5). The ranges with a high content of Ca also have high contents of Mn and, particularly, Sr (Table 5). In the range 55–110 cm, the content of Sr is twice as high as its clarke content, and in the 136 cm horizon (with a high content of aragonite), it is abnormally high, 3800 ppm.

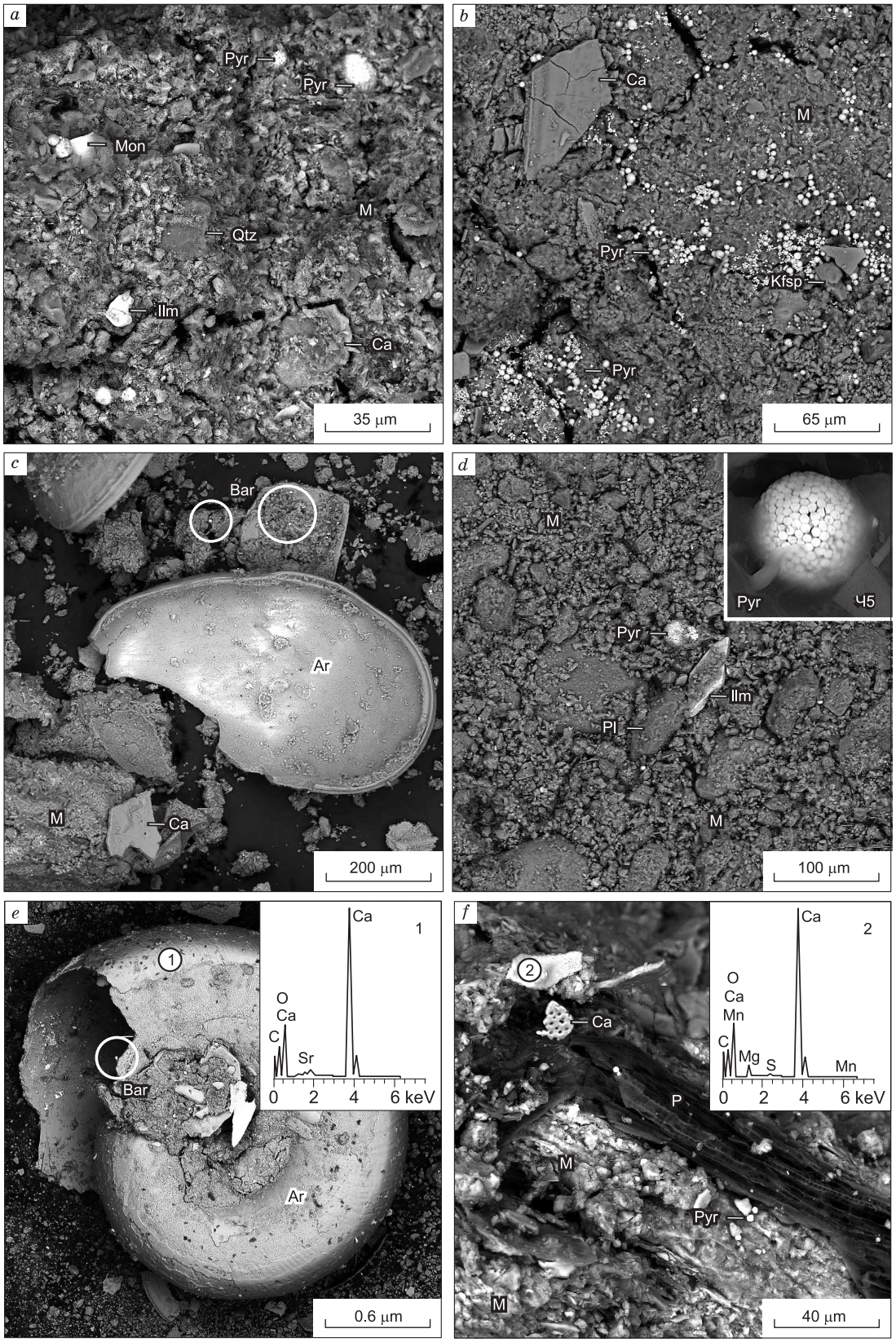


**Fig. 5.** Photomicrographs of the Itkul' sediments from the depth ranges: *a*, 0–2 cm; *b,* 105–110 cm; *c*, 136–138 cm (an ostracode shell is seen); *d*, 145–150 cm; spectra of a mollusk shell (*e,* 1) from a depth of 145 cm and of authigenic calcite (*f*, 2) from a depth of 10 cm. Minerals: Bar, barite, Ca, calcium carbonate, Mon, monazite, Pyr, pyrite framboids and crystals. Other mineral names follow Fig 4. M, carbonate-argillaceous substance (marly clay), R, plant remains (Photomicrographs were made by E.V. Lazareva using a TESCAN MIRA 3 LMU scanning electron microscope).

**Table 5.** Distribution of chemical elements throughout the section of the Itkul' bottom sediments

| Depth, cm | Ash content, % | Fe | Al | Ca | Mg | K | Na | Sr | Mn | Zn | Co | Ni | Cu | Pb | Cd | Cr | Be | Li | As | Hg |
|---|---|---|---|---|---|---|---|---|---|---|---|---|---|---|---|---|---|---|---|---|
| | | % | | | | | | ppm | | | | | | | | | | | | |
| 1 | 90.0 | 2.45 | 4.18 | 10.5 | 1.6 | 1.4 | 0.98 | 1120 | 799 | 60 | 9.4 | 28 | 21 | 9.5 | 0.067 | 65 | 0.8 | 24 | 7.8 | 0.018 |
| 4 | 88.4 | 2.62 | 4.76 | 7.9 | 1.8 | 1.7 | 0.90 | 729 | 789 | 66 | 9.8 | 30 | 23 | 11.6 | 0.058 | 70 | 0.8 | 23 | 4.8 | 0.019 |
| 10 | 86.4 | 2.59 | 4.42 | 6.1 | 1.7 | 1.6 | 1.10 | 481 | 745 | 64 | 9.3 | 30 | 23 | 12.1 | 0.064 | 73 | 1.3 | 24 | 5.0 | 0.028 |
| 14 | 88.0 | 2.61 | 4.42 | 6.8 | 1.7 | 1.6 | 1.00 | 563 | 747 | 64 | 9.3 | 30 | 22 | 11.7 | 0.064 | 87 | 1.4 | 23 | 4.4 | 0.018 |
| 18 | 88.2 | 2.62 | 4.74 | 6.3 | 1.8 | 1.7 | 1.00 | 490 | 749 | 66 | 9.8 | 31 | 23 | 11.6 | 0.063 | 67 | 1.5 | 24 | 5.8 | 0.011 |
| 25 | 88.1 | 2.61 | 4.54 | 6.2 | 1.7 | 1.7 | 0.98 | 470 | 751 | 64 | 10.5 | 32 | 24 | 12.5 | 0.058 | 73 | 2.2 | 25 | 10.0 | 0.016 |
| 35 | 86.4 | 2.97 | 5.23 | 6.2 | 1.9 | 1.8 | 1.30 | 423 | 774 | 67 | 10.7 | 32 | 25 | 12.7 | 0.080 | 68 | 1.1 | 24 | 7.1 | 0.027 |
| 45 | 87.7 | 2.93 | 5.03 | 6.8 | 1.7 | 1.9 | 0.93 | 493 | 758 | 69 | 9.9 | 32 | 25 | 12.5 | 0.089 | 66 | 1.3 | 26 | 7.2 | 0.028 |
| 55 | 88.2 | 2.26 | 4.03 | 8.7 | 1.7 | 1.5 | 0.72 | 1098 | 776 | 55 | 7.5 | 25 | 21 | 9.0 | 0.080 | 52 | 1.2 | 23 | 9.7 | 0.026 |
| 75 | 85.7 | 2.44 | 3.66 | 11.8 | 1.3 | 1.2 | 0.69 | 1327 | 841 | 52 | 8.6 | 23 | 19 | 8.0 | 0.072 | 59 | 1.1 | 22 | 8.1 | 0.015 |
| 95 | 90.7 | 2.01 | 4.02 | 12.0 | 1.2 | 1.7 | 0.69 | 981 | 834 | 57 | 6.6 | 22 | 22 | 8.0 | 0.084 | 67 | 1.1 | 21 | 8.2 | 0.013 |
| 110 | 88.1 | 1.57 | 2.91 | 16.4 | 1.1 | 0.9 | 0.55 | 1259 | 999 | 49 | 6.3 | 20 | 17 | 5.1 | 0.097 | 49 | 0.6 | 18 | 8.0 | 0.024 |
| 130 | 94.2 | 2.80 | 4.60 | 3.7 | 0.9 | 2.5 | 1.33 | 336 | 332 | 67 | 9.3 | 32 | 27 | 11.1 | 0.110 | 72 | 1.7 | 26 | 15.9 | 0.029 |
| 136 | 85.6 | 1.00 | 0.68 | 22.0 | 0.8 | 0.2 | 0.30 | 3800 | 628 | 29 | 8.3 | 12 | 11 | 1.0 | 0.069 | 38 | 0.2 | 31 | 12.3 | 0.030 |
| 140 | 91.1 | 2.07 | 3.82 | 13.3 | 1.1 | 1.4 | 0.66 | 989 | 849 | 48 | 8.5 | 24 | 20 | 6.9 | 0.079 | 59 | 1.2 | 20 | 9.6 | 0.031 |
| 145 | 93.5 | 2.75 | 4.34 | 1.8 | 1.1 | 2.7 | 1.30 | 182 | 249 | 72 | 10.5 | 34 | 29 | 12.3 | 0.086 | 84 | 1.6 | 27 | 17.0 | 0.021 |
| 150 | 90.5 | 2.96 | 4.60 | 2.9 | 1.0 | 2.4 | 1.20 | 263 | 296 | 69 | 9.8 | 33 | 24 | 11.2 | 0.086 | 72 | 1.3 | 25 | 9.8 | 0.024 |
| 160 | 95.5 | 2.72 | 5.56 | 6.8 | 1.1 | 2.0 | 1.30 | 197 | 809 | 60 | 9.2 | 29 | 16 | 12.9 | 0.150 | 53 | 1.6 | 23 | 8.3 | 0.026 |
| 175 | 85.5 | 2.90 | 5.14 | 6.0 | 1.9 | 1.7 | 1.30 | 387 | 774 | 67 | 10.6 | 32 | 23 | 11.9 | 0.130 | 66 | 1.3 | 24 | 7.9 | 0.008 |
| Sh | – | – | – | – | 0.2 | – | – | 1460 | 67 | 9.4 | – | – | 4.7 | – | – | – | – | – | – | – |

Note. Ash content was determined at 450 °C. Sh, mollusk shells from the depth range 145–160 cm. Dash, not analyzed. The bulk contents of chemical elements were determined by AAS at the Analytical Center for Multi-Elemental and Isotope Research of V.S. Sobolev Institute of Geology and Mineralogy, Novosibirsk (analysts V.N. Il'ina and N.V. Androsova). The content of Hg was determined by the "cold steam" method with amalgamation of the element on a gold sorbent (analyst Zh.O. Badmaeva).

The main source of Mg present in the sediments is its supply with clay minerals from the lake drainage area, which is well confirmed by the similar distribution of Mg, Si, and Al throughout the sediment column (Tables 4 and 5). Chlorite, amphibole, and kaolinite ubiquitous in the sediment section might also be the source of terrigenous Mg. Magnesian calcite precipitated from the lake water might be an additional (authigenic) source of Mg.

Correlation analysis revealed three groups of chemical elements according to their distribution throughout the bottom sediment section. On calculation, we ignored the sample taken at a depth of 138 cm, because it differs significantly from the other in the low contents of Fe, Al, K, Ni, Cu, and Pb and extremely high contents of Sr, Ca, and Li. As seen from the R-type analysis data (Fig. 7*a*), all 19 variables are divided into three groups according to the degree of correlation: Fe–Pb–Al–Na+Zn–Ni–Li–Co (conditionally alkaline); (2) K–Cd–Hg–As–Be–Cu–Cr; and (3) Mg–Mn–Sr–Ca (conditionally basic), showing a weak negative correlation with two other groups. The analysis showed a high degree of correlation of Fe, Na, and Al with Mn, Mg, Ca, and Sr. This provides an objective explanation of the division of the sediment samples into three groups (Fig. 7*b*). The deep horizons of the bottom sediments are characterized by low contents of Ca, Mg, Sr, and Mn but extremely high contents of Fe, Al, Na, and As. The middle horizons, on the contrary, have high contents of Ca and Mn. The samples taken in the upper horizons show a specific trace-element patterns and high contents of Al and Fe.

We have established a positive correlation among Ca, Sr, and Mn and their positive correlation with carbonates (0.62–0.66) and strong negative correlation (–0.96 to –0.77) with Al, Fe, K, Na, Ni, Zn, Cu, Pb, Cr, and Be. The analysis data show a strong positive Ca–Sr correlation (0.89), a weak Ca–Mn correlation (0.52), and almost no Ca–Mg correlation (–0.35). A strong negative correlation is observed for the pairs Ca–Ni (–0.96), Ca–Fe (–0.93), Ca–K (–0.92), Ca–Na (–0.90), and Ca–Al (–0.85).

Enrichment factors (EF). The calculated EF values for the averaged elemental composition of different beds of the Itkul' sedimentary strata (Fig. 8) indicate that the contents of Fe, K, Na, and Mg are close to those in argillaceous shale (Li, 1991), which is explained by the marly clay composition of the sediments. At the same time, the sediments are depleted in Li and Be. In contrast to sapropel Lakes Bolshie Toroki and Minzelinskoe studied earlier (Mal'tsev et al., 2014a,b), the Itkul' sediments, poor in organic matter, are not enriched in Cu and Zn in the upper bed. In the above

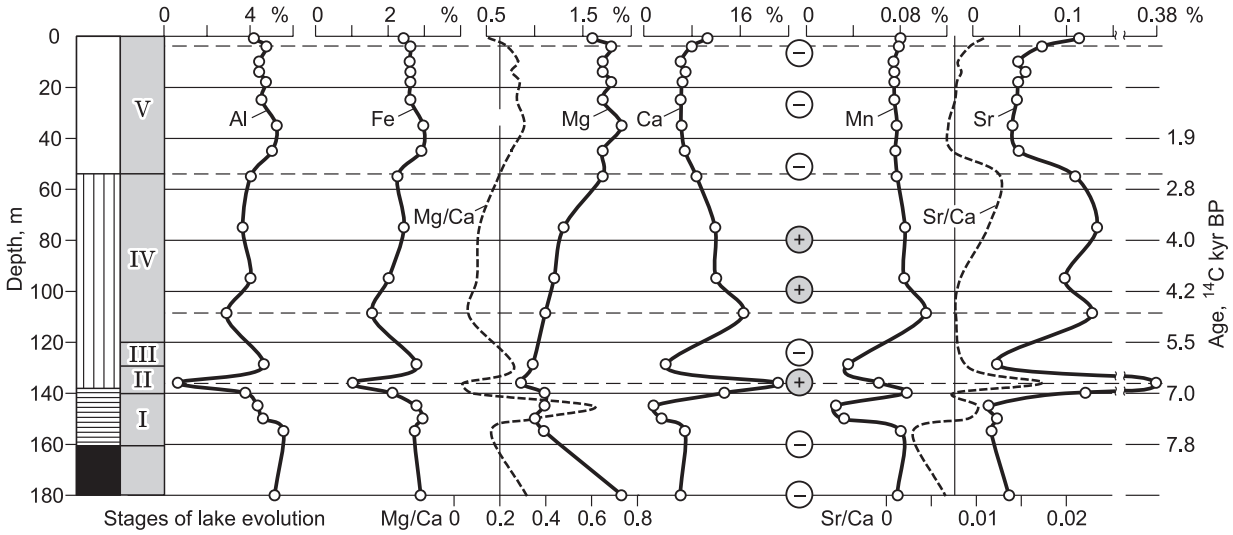


**Fig. 6.** Distribution of chemical elements throughout the Itkul' bottom sediment column. "+", the presence of aragonite in the sediments (XRD data), "–", the absence of aragonite. Designations follow Fig. 2. The stages of the lake evolution are described in the text.

study we explained the high contents of these elements in the upper beds of sapropels mostly by their supply with OM.

The EF data show that all beds of the Itkul' sedimentary strata are significantly enriched in Ca and Sr and the high-carbonate range 136–138 cm is additionally enriched in Mg and Mn (Fig. 8). The enrichment of the sediments in Sr is due to its presence in carbonates, in particular, calcite and, especially, aragonite. Aragonite is known to be on average 20–30 times richer in Sr than calcite (Yudovich et al., 1980; Yudovich, 2007; Yudovich and Ketris, 2011). The Mg enrichment of the sediments at a depth of 136 cm is due to a significant domination of Mg-$CaCO_3$ over $CaCO_3$, which is observed only in this part of the section (Fig. 4).

**The sources of Ca.** We calculated the contents of authigenic ($Ca_{auth}$) and terrigenous ($C_{ter}$) calcium in the Itkul' bottom sediments (Fig. 9). Authigenic calcium in the sediments is chemogenic (precipitated from the lake water) and biogenic (mollusk shells). Terrigenous calcium is of "mixed" nature and is present in (1) carbonates of the lake drainage area and (2) clay minerals of the sediments. The average content of $Ca_{ter}$ over the sediment section is 1.7%, which is close to the content of Ca in argillaceous shale (1.6%) (Li, 1991). The maximum content, 2.1%, was established in the lower depth range of the sediments (150–160 cm), and the minimum one, 1.1%, in the range 107–114 cm. The average content of $Ca_{auth}$ over the section is 7%. The minimum content, 0.1%, is in the depth range 145–150 cm, where carbonates did not precipitate in the lake at the initial stage of its formation and Ca was supplied from terrigenous sources. A higher content of $Ca_{auth}$, 11.7%, is observed in the middle part of the section, and the maximum content, 20.5%, in the range 136–138 cm. At a depth of 130 cm, the content of $Ca_{auth}$ drastically decreases, to 1.7%, whereas the content of $Ca_{ter}$ increases to 2.0%. The upper third of the section is characterized by a reduced content of $Ca_{auth}$, ~5%, and in the subsurface sediments it increases to ~10%.

**Radioactivity.** The data on the radioactivity of the upper sediment beds show an abnormal decrease in the content of $^{210}Pb$ toward the upper depth ranges. Its content is in general low, 26.6–20.5 Bq/kg (Table 6). Isotope $^{238}U$ is evenly dis-

**Table 6.** Radioactivity of the upper (0–20 cm) bed of the Itkul' sediments

| Depth, cm | $^{238}U$, ppm | $^{238}U$ | $^{210}Pb$ | $^{226}Ra$ | $^{232}Th$ | $^{232}Th$ | $^{137}Cs$ | $^{40}K$ |
|---|---|---|---|---|---|---|---|---|
| | | Bq/kg | | | | Bq/kg | | |
| 2 | 2.3 | 28.4 | 20.5 | 22.7 | 6.5 | 26.3 | 0.1 | 359 |
| 4 | 2.4 | 30.3 | 25.9 | 31.7 | 7.1 | 29.0 | 0.0 | 377 |
| 20 | 2.8 | 34.7 | 26.6 | 30.5 | 7.7 | 31.4 | 0.0 | 407 |

Note. Radioactivity was measured on a low-background gamma spectrometer with a coaxial well-type HPGe detector (analyst M.S. Mel'gunov).

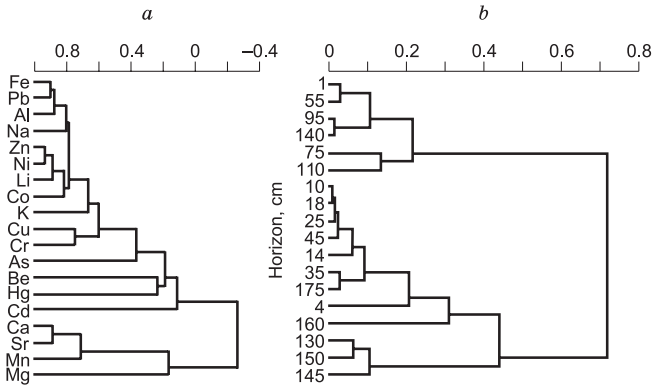


**Fig. 7.** Correlation analysis. *a*, Degree of correlation between variables and groups of variables (contents of chemical elements in the sediments); *b*, grouping of chemical analyses of the Itkul' sediment samples by the cluster method. The upper line is the scale of correlation coefficients: *a*, *R*-type analysis; *b*, Q-type analysis.

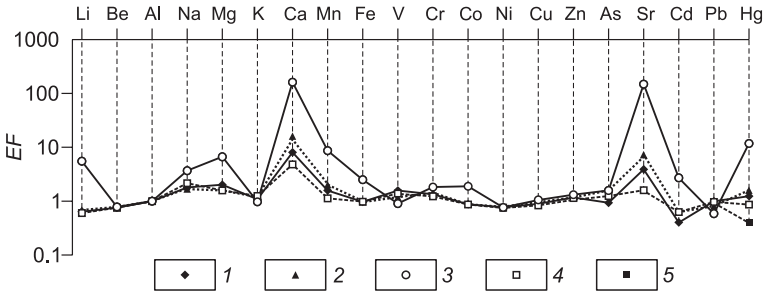


**Fig. 8.** Enrichment factors (*EF*) of chemical elements in the Itkul' bottom sediments in the depth ranges: *1*, 0–55 cm; *2*, 55–136 cm; *3*, 136–138 cm (light interbed with shell remains); *4*, 138–162 cm; *5*, 162–180 cm. Normalized to the contents of Al and clarke contents of elements in argillaceous shales (Li, 1991).

tributed throughout the sediment section and amounts to 2.8–2.3 ppm. The content of $^{226}$Ra is 30.5–22.7 Bq/kg and decreases toward the upper depth ranges. Note that the contents of $^{238}$U and $^{226}$Ra in the Itkul' sediments are an order of magnitude higher than those in the sapropel of earlier studied Lake Minzelinskoe (Mal'tsev et al., 2014b). Apparently, this is due to a large amount of clay minerals in the Itkul' sediments and a small amount of organic matter. The content of $^{137}$Cs in the Itkul' sediments is below its detection limit.

**Forms of element occurrence.** Lithophile elements Al, K, and Na are present mostly in residual minerals of the Itkul' sediments, such as quartz, feldspars, plagioclase, amphibole, kaolinite, and mica (Fig. 10). Iron is present as part of organic matter and as sulfides, but since the content of OM in the sediments is low ($C_{org}$ = 4–9%), iron occurs predominantly in pyrite identified by XRD (Fig. 4) and SEM (Fig. 5). A minor amount of iron in the form of carbonates was found in the depth range 95–100 cm. Calcium and strontium are present mainly as their carbonates; in the depth range 135–140 cm, the portions of Ca and Sr oxides and hydroxides highly increase. Magnesium occurs in diverse forms, with its carbonates being scarce and its residual minerals being, on the contrary, abundant, which is due to the argillaceous composition of the bottom sediments. In the depth range 95–100 cm, a slight increase in the content of Mg carbonates is observed. The range 135–140 cm is characterized by the highest contents of Mg carbonates (calculated on the total Mg basis) in the section. Manganese occurs mainly as its carbonates, but, following the stepwise leaching process, Mn oxides and hydroxides partly dissolve at the carbonate formation stage; therefore, oxidized Mn compounds can also be present in the sediments.

## DISCUSSION

**Mineral and geochemical indicators in the reconstruction of the lake evolution.** Lake Itkul' formed in the middle Holocene at 7.8 $^{14}$C kyr BP (8.8 cal ka), under the influence of a rapid and drastic change of the cold arid climate by the warm humid one (Treshnikov, 1986). After the melting of a glacier, a lake began to form at the place of loess-like loams.

I. At the initial stages of the lake formation (Fig. 6), at ~7.8–7.0 $^{14}$C kyr BP, silicate material (quartz, K-feldspar, mica, chlorite, and kaolinite) actively accumulated in the depth range 162–145 cm of the bottom sediments. This interval has the highest contents (wt.%) of $SiO_2$ (57), $Al_2O_3$ (14), and $K_2O$ (3) supplied into the lake mostly with terrig-

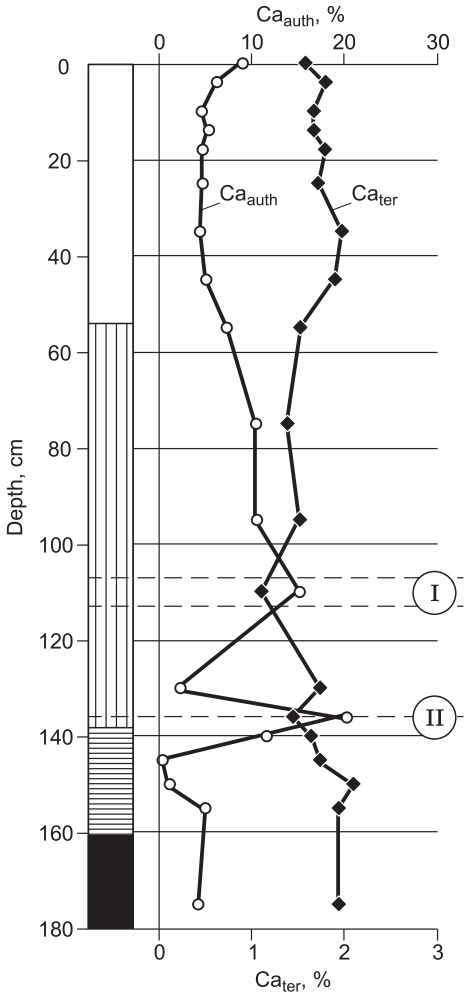


**Fig. 9.** Distribution of Ca throughout the Itkul' bottom sediment column. $Ca_{auth}$, authigenic calcium (chemogenic and biogenic), $Ca_{ter}$, terrigenous calcium. Designations follow Fig. 2.

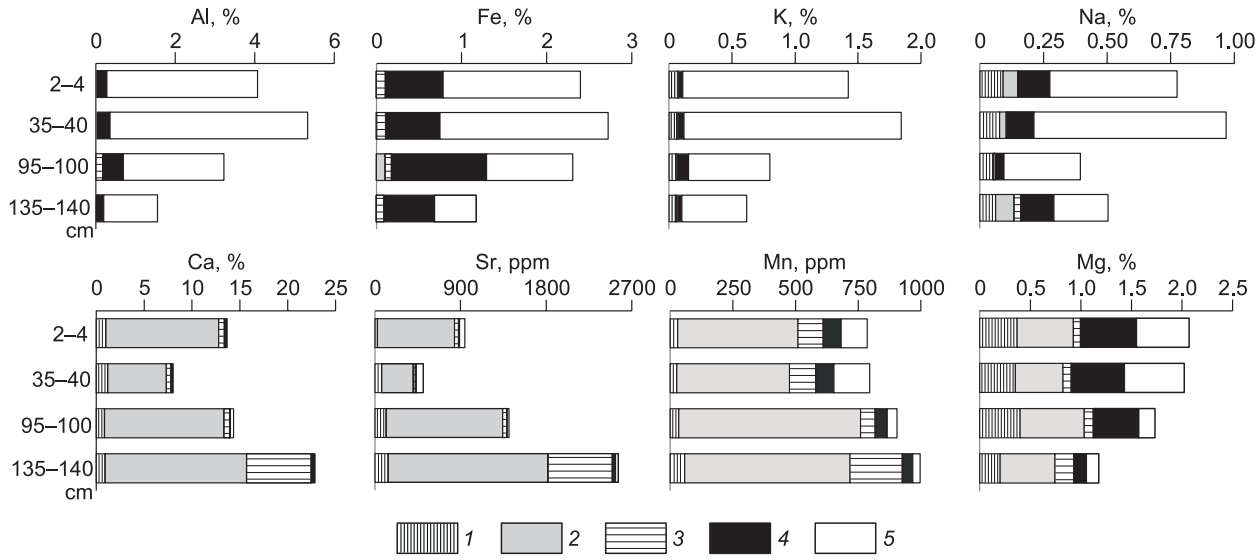


**Fig. 10.** Forms of element occurrence in different depth ranges of the Itkul' sediments: *1*, exchange ions; 2, carbonates (for Mn, oxides and hydroxides as well); *3*, oxides and hydroxides; *4*, organic matter and sulfides; *5*, residual (solid) substances.

enous products of destruction of Quaternary blanket deposits. All this indicates the high standing of the lake water and an active terrigenous supply from the drainage areas into the lake. At the high water level and low salinity of the lake, carbonates (calcites with a minimum impurity of Mg) poorly precipitated. The absence of Mg-calcites from this lowest range of the bottom sediments might be due to diagenetic transformations of carbonates, in which Mg-calcite transforms into more stable low-Mg calcite. However, it is most likely that the change in the Mg content of calcite reflects the changes in climate humidity and water content of the lake. Lowly magnesian calcite precipitates from the subsaline lake water moderately saturated with carbonates (Nechiporenko and Bondarenko, 1988). It is at the stage of the Lake Itkul' formation (depth range 162–145 cm), during the high water level and low salinity, that the water lacked Mg-calcites and had low total contents of carbonates.

II. At the stage of the lake shallowing (depth range 145–130 cm), ~7.0 $^{14}$C kyr BP, with a significant development of biota (mollusks), the contents of Mg-calcites and aragonites reached their maxima on the background of an increase in $C_{org}$ content to 7.1%. The depth range 136–138 cm corresponds to the maximum shallowing of the lake throughout its evolution. This is confirmed by the highest contents of carbonates and by domination of aragonite over calcites and of Mg-calcite over $CaCO_3$ in this interval. Traces of gypsum in it indicate a strong shallowing of the lake and an increase in its salinity. Gypsum can precipitate at the initial stage of halogenesis, when water becomes saturated with NaCl. The maximum contents of Sr in the range 136–138 cm also reflect a strong shallowing of the lake. The contents of Mg in this range decrease less than the contents of Al, K, Na, and Fe, whereas the content of Ca drastically increases, which testifies to the active precipitation of Mg-calcites at the shallow-water stage of the lake evolution, when the produced chemogenic carbonates, mainly Mg-$CaCO_3$, contained most of the total Mg. This is confirmed by the data on the forms of Mg occurrence, showing the maximum portion of Mg carbonate in the range 136–138 cm as compared with the rest section. The most active precipitation of carbonates in this range is evidenced by the maximum increase in the content of $Ca_{auth}$ and by the highest total contents of Ca.

Upsection (depth range 130–0 cm), we observe a tendency for a slow stepwise rise in the lake water level and for the lake freshening. This process was accompanied by periodical slight fluctuations from shallowing to watering of the lake.

III. After the shallowing of the lake at ~7 $^{14}$C kyr BP, there was a rapid rise in its water level at 7.0–5.5 $^{14}$C kyr BP (depth range 130–125 cm). This range is characterized by a decrease in the contents of carbonates. A drastic drop in the contents of Ca and Sr in the range 130–120 cm on the background of an increase in the contents of Al and Fe indicates a rise in the lake water level. This rise is confirmed by higher contents of "Al group" elements, reflecting a more intense terrigenous input. The drastic decrease in the content of $Ca_{auth}$ to 1.7% on the background of the increase in the content of $Ca_{ter}$ to 2.0% at a depth of 130 cm also confirms a rise in the lake water level.

IV. At ~5.5–2.8 $^{14}$C kyr BP, the lake water level fell (depth range 125–55 cm) as a result of the water evaporation and a less intense water inflow, which led to a higher lake salinity. Thus, the conditions became favorable for the precipitation of carbonates; this was reflected in the increased contents of Ca in the sediments. Note that the depth range 120–100 cm (5.5–4.3 $^{14}$C kyr BP) is characterized by the maximum shallowing of the lake over the period 5.5–2.8 $^{14}$C kyr BP. The increase in the contents of Ca and Sr and the decrease in the contents of Mg and Al in the depth range

120–55 cm might indicate changes in the lake water parameters (salinity, carbonate alkalinity, pH, and temperature) and, hence, a more active chemogenic precipitation of calcium carbonates from the Mg-poor water. According to Yudovich et al. (1980), an increase in the water salinity led to the accumulation of Sr. Chemogenic carbonates became enriched in Sr, which is confirmed by the significant Sr enrichment of this horizon as compared with the underlying ones. The amount of Mg-calcites in it is smaller than that at the previous shallowing stage (depth range 140–130 cm). This indicates a smaller shallowing of the lake than that marked in the depth range 136–138 cm. The range 120–100 cm is characterized by the maximum (for this stage) drop in water level and an increase in water salinity: domination of Mg-$CaCO_3$ over $CaCO_3$, a drastic increase in the content of carbonates, and the absence of aragonite. The contents of Al and Fe significantly decrease on the background of the stable contents of Mg and a drastic increase in the contents of Ca and organic matter (Fig. 2). In the depth range 120–55 cm, the increase in the content of Ca is not accompanied by an increase in the content of Mg (the latter, on the contrary, decreases, although calcites become more magnesian with depth). This is explained by the low portion of Mg in carbonates, because most of it is present in clay minerals.

V. An increase in the lake water level and a decrease in water salinity (depth range 55–0 cm, 2.8–0 $^{14}C$ kyr BP) strongly restrained carbonate formation (and, hence, led to a decrease in the content of Ca in the sediments) on the background of an intense inflow of terrigenous components ($SiO_2$ and $Al_2O_3$). At this stage of the lake watering, the contents of Ca and carbonates in the sediments decreased, which was expressed as a significant decrease in the portion of Mg-$CaCO_3$ and the absence of aragonite. A terrigenous input increased, as evidenced by much higher contents of Al, Fe, Mg, and Na (Fig. 6, Table 5) and a higher content of $Ca_{ter}$ as compared with the underlying sediment intervals.

The composition of sediments formed at the current stage of the lake evolution (10–0 cm, the last ~100 yr) shows an increase in water salinity and in the contents of Ca and Sr in the sediments and a slight increase in the amount of Mg-$CaCO_3$. Hence, the lake tends for the next shallowing.

We have established that the Mg/Ca and Sr/Ca ratios in the bottom sediments, which depend on the Mg/Ca and Sr/Ca ratios in the lake water (Sklyarov et al., 2010; Solotchina et al., 2012), change downsection (Fig. 6). The Sr/Ca ratio, an indicator of water salinity (Ricketts et al., 2001; Schwarz et al., 2017), increases in the middle depth range (100–55 cm) of the sedimentary strata, especially in the range 138–136 cm, which indicates the maximum salinity of the lake water in the corresponding periods. There is also a positive Sr/Ca trend in the uppermost sediment intervals (10–0 cm), which points to a current increase in water salinity. The Mg/Ca ratio determining the type of precipitating carbonates does not increase downsection (55–110 cm) despite the presence of Mg-calcites. This is apparently because calcites in the mentioned depth range are lowly magnesian.

**Geochemistry of Sr and Mn in the carbonate sediments.** The data on the forms of Sr and Mn occurrence in the lacustrine sediments show that these elements are present mostly in carbonates. This phenomenon is well described elsewhere (Mitterer, 1972; Yudovich et al., 1980; Ambatsian et al., 1997; Yudovich and Ketris, 2011; Kuznetsov, 2013) and is due to different factors, e.g., the similar ionic radii of Ca and Sr and the redox potential of the medium for Mn.

The migration capability of Sr in hypergenesis zone is determined by its ionic radius commensurate with that of Ca, which often leads to the isostructural replacement of Ca by Sr in calcites (Yudovich and Ketris, 2011). This fact is confirmed by a positive correlation between the contents of Ca and Sr in the Itkul' sediments (Fig. 11). The maximum content of Sr (0.38%) is found in the depth range 136–138 cm, where aragonite considerably dominates over calcite, according to the XRD data. The Sr enrichment of aragonite in Lake Itkul' is due to the fact that ions $Sr^{2+}$ in the crystal lattice are mostly octa-coordinated; therefore, aragonite having a rhombic syngony (in contrast to trigonal calcites) is especially enriched in Sr (Yudovich and Ketris, 2011; Kuznetsov, 2013). As seen from the XRD data (Figs. 4 and 6), the drastic increase in the content of Sr (exceeding its clarke content) in the depth ranges 55–110 and 136–138 cm matches the appearance of aragonite. Thus, we assume that it is aragonite that provides high contents of Sr in the sediments.

Aragonite in the Itkul' sediments can be from two sources, chemogenic and biogenic (mollusk shells). The studied mollusk shells from the lower beds of the sediments consisted mostly of aragonite (Fig. 4*c*), in contrast to marine shells with a calcite composition (Hallam and Price, 1968; Kennedy et al., 1969; Yudovich et al., 1980; Demina and Os'kina, 2012). In addition to aragonite, the shells contain

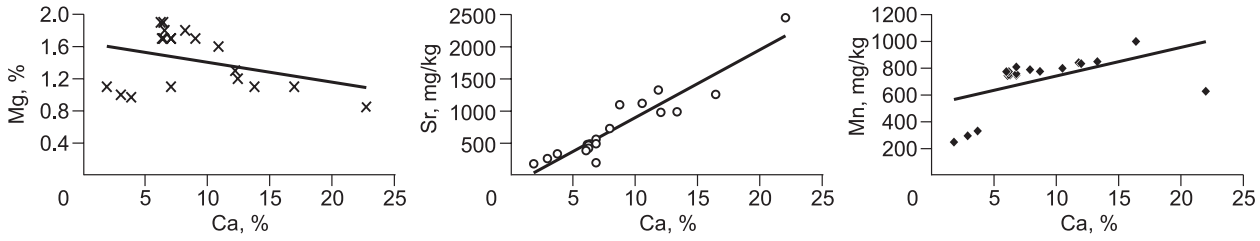


**Fig. 11.** Contents of Mg, Sr, and Mn vs. contents of Ca in the Itkul' sediments.

an impurity of Mg-calcite. The geochemical data show (Table 5) that the shells contain 0.14% Sr (four times higher than its clarke content), 0.22% Mg, and a minor amount of Mn (67 ppm). At a first glance, the mollusk shells can explain the origin of aragonite in the Itkul' sediments and, hence, their enrichment in Sr. However, the depth ranges containing fragments of shells (145–160 cm) do not coincide with the sediment intervals where aragonite was revealed by XRD (80–100 and 136–138 cm). Therefore, the presence of aragonite in the depth range 80–100 cm and its largest amount in the range 136–138 cm have only one explanation, namely, the chemogenic precipitation of aragonite from the highly saline water under significant shallowing of the lake.

Chemical precipitation of aragonite is not typical of freshwater reservoirs of humid zones (Kholodov, 2006). Aragonite in the surface water of fresh lakes is metastable and usually does not precipitate; variably magnesian calcite precipitates instead of it. Aragonite commonly forms at great depths (in seas and oceans), at high pressures and high temperatures (Reeder, 1983). There might be exceptions, however. As shown earlier (Leeder, 1982; Nechiporenko and Bondarenko, 1988; Solotchina et al., 2013), aragonite can precipitate at shallow depths in water with a high concentration of magnesium ions (e.g., in salt lakes). Under such conditions, ions $Mg^{2+}$ surrounded by a dense hydrate shell ($[Mg(H_2O)_6]^{2+}$) are strongly adsorbed by calcite (Berner, 1975; Solotchina et al., 2013). The crystal–solution equilibrium is determined by the ion exchange at the crystal surface, and if the entire calcite surface is covered with a layer of adsorbed Mg, then a $CaCO_3$ crystal behaves like a magnesite crystal (Reeder, 1983). Since the solution is not saturated with $MgCO_3$, magnesite cannot grow. The solution, however, should get rid of excess $CaCO_3$; therefore, aragonite crystals can grow. Hydrated magnesium ions adsorb on aragonite much worse because of its specific rhombic structure. Therefore, their adsorption has little effect on the rate of aragonite crystallization (Nechiporenko and Bondarenko, 1988; Solotchina et al., 2013). Apparently, precipitation of aragonite took place in Lake Itkul' at the stage of its maximum shallowing and increase in its mineralization on the background of increasing concentrations of $Mg^{2+}$ (depth range 136–138 cm). The maximum *EF* values and Sr/Ca ratio in the depth range 136–138 cm are indirect evidence for high concentrations of $Mg^{2+}$ in the water in that period. This indicates a drastic increase in water salinity at that time. We also revealed a large amount of Mg-calcite in the above depth range.

Thus, an increase in water salinity and a high concentration of $Mg^{2+}$ might have led to the precipitation of Mg-calcite and, then, aragonite. An increase in water salinity as a result of the lake shallowing and the increased total carbonate alkalinity favored precipitation of Mg-calcite. The subsequent shallowing, increase in mineralization (causing metamorphization of water, according to the evaporative-concentration mechanism), and increase in the content of $Mg^{2+}$ led to the precipitation of aragonite. Based on the report by Last (2002), Solotchina et al. (2012) described a similar sequence of the precipitation of Mg-calcite and aragonite in salt lakes, reflecting an increase in the Mg/Ca ratio and salinity of the water: low-Mg calcite–high-Mg calcite–aragonite–dolomite–magnesite/huntite.

As for Mn, its incorporation into the carbonate structure is strongly affected by the redox potential of the medium, because manganese must be in a divalent state to replace Ca. In a highly oxidizing environment, such as lake water or upper oxidized beds of sediments, Mn ions (predominantly $Mn^{4+}$) cannot be present in the carbonate phase. The redox potential gradually shifts toward reducing conditions only as the sediments become more and more isolated from surface oxygen. This shift is accompanied by the enrichment of carbonates with Mn (Ambatsian et al., 1997; Kuznetsov, 2013). In Lake Itkul', however, reducing conditions (Eh = –171 mV) are observed already in the first 10 cm of the sediments. At the initial stages of carbonate formation, part of reactive (mobile) Mn here can enter the structure of carbonates formed at the water–sediments interface. Note that the alkaline water (pH = 9.1) of Lake Itkul is not favorable for the migration of most metals, which can precipitate as poorly soluble carbonates already at the stage of sediment genesis (Perel'man, 1982). Data on the chemical composition of pore water in the carbonate sediments of Lake Bol'shie Toroki (Mal'tsev et al., 2014b) showed that manganese is present in their upper strata mostly as Mn (II) (up to 90%). Therefore, Mn can replace Ca in carbonates both at the stage of sediment genesis and at the early stage of diagenesis. This agrees with the strict linear correlation between the contents of Mn and Ca (Fig. 11). The XRD analysis revealed no own Mn-minerals in the sediments (Fig. 4). The EPR analysis confirmed that the Itkul' carbonates contain 189 to 422 mg/kg Mn, which amounts to 23–55% of its total content in the lacustrine sediments (Table 7). Note that the sediment horizons containing aragonite (136–138 cm) have a lower total content of Mn than the "calcite" zones (Table 5). The possible reason is that manganese does not enter the crystalline structure of aragonite, which is confirmed by literature data (Yudovich and Ketris, 2011, 2014). The analysis of mollusk shells composed of aragonite also shows that their content of Mn is an order of magnitude lower (67 ppm) than the total content of Mn in the sediments (710 ppm). The SEM data confirm that the mollusk shells and ostracodes are free of Mn.

**Geochemistry of Pb and $^{210}$Pb.** The upper horizons of the sediments do not show an increase in the total content of Pb and the content of $^{210}$Pb marking the anthropogenic impact on the environment over the past 100 years. There is only one explanation for this fact: Technogenous lead supplied from the atmosphere into the Itkul' water with high pH (9.1) transforms into dissolved bicarbonate $Pb(HCO_3)_2$ and does not accumulate in the sediments. The observed increase in the content of $^{210}$Pb downsection (Table 6) (although the opposite pattern should be observed, i.e., a decrease in the

**Table 7.** Content of Mn in carbonates from different depth ranges of the Itkul' sediments

| Depth range, cm | Content of Mn in carbonates, mg/kg | Bulk content of Mn, mg/kg | Portion of carbonate-associated Mn of total Mn, % | Carbonates, % | Proportions of mineral phases of Ca |
|---|---|---|---|---|---|
| 2–4 | 256 | 799 | 32.0 | 29.4 | $CaCO_3$ > Mg-Cal |
| 35–40 | 422 | 774 | 54.5 | 20.7 | $CaCO_3$ > Mg-Cal |
| 95–100 | 189 | 834 | 22.7 | 37.6 | $CaCO_3$ > Ar > Mg-Cal |
| 135–140 | 251 | 628 | 39.9 | 55.3 | Ar > Mg-Cal > $CaCO_3$ |

Note. Mg-Cal, magnesian calcite; Ar, aragonite. Contents of Mn in carbonates were determined by EPR (analyst D.V. Stas'). The bulk contents of Mn were determined by AAS (analysts V.N. Il'ina and N.V. Androsova). Mineral phases of Ca were identified by XRD (analyst L.V. Miroshnichenko).

content of $^{210}$Pb because of its decay) is apparently due to a change in pH. The drop in pH from 9.1 to 8.2 in the sediments (as compared with the lake water) decreases the mobility of Pb in deeper horizons. As a result, Pb is less easily leached from the solid phase into the pore water downsection. Therefore, lead insignificantly accumulates in the deeper horizons of the bottom sediments.

Thus, most of the lead accumulating in the Itkul' sediments is terrigenous (poorly mobile); it is supplied with clay particles into the lake, which is confirmed by the similar distribution patterns of total Pb and Al, K, and Fe (Table 5). In contrast, $^{210}$Pb arriving at the lake from the atmosphere as a result of anthropogenic pollution does not accumulate in the sediments and transforms into dissolved bicarbonate. This phenomenon calls for a more detailed study.

## CONCLUSIONS

(1) The bottom sediments of Lake Itkul' are characterized by a heterogeneous chemical composition, different distributions of Al, Fe, Na, K, Mg, Ca, Sr, Mn, Cu, Zn, Pb, and carbonates throughout the section, and different contents of Mg in calcites, which is mostly due to changes in the sediment genesis environments and to the rise or fall in the lake water level. At the stages of the lake shallowing, the conditions were favorable for the precipitation of carbonates, which led to an increase in the contents of Ca, Sr, and Mn in the sediments. At the stages of the water level rise, the terrigenous input from the lake drainage area intensified, and thus the contents of Si, Al, Fe, Na, and K in the sediments increased.

(2) The sedimentary strata of the lacustrine bottom sediments formed in the middle Holocene over a period of 7.8 $^{14}$C kyr BP (8.8 cal kyr BP). Lake Itkul' passed through the following stages of evolution: (1) the beginning of sedimentation, 7.8–7.0 $^{14}$C kyr BP; (2) extreme shallowing with a probable complete drying, ~7.0–5.5 $^{14}$C kyr BP; (3) rise in the water level, ~5.5–4.3 $^{14}$C kyr BP; (4) repeated shallowing, 4.3–2.8 $^{14}$C kyr BP; and (5) subsequent watering, 2.8–0 $^{14}$C kyr BP, with a tendency for shallowing at present. The stages of strong shallowing of the lake are characterized by an increase in the Mg content of calcites and by the presence of aragonite in the sediments.

(3) At the stage of the maximum shallowing of the lake at ~7 $^{14}$C kyr BP, the conditions were favorable for the precipitation of aragonite. An increase in water salinity and a high concentration of $Mg^{2+}$ led to the active precipitation of aragonite and Mg-calcite. The increasing water salinity and total carbonate alkalinity led to the precipitation of Mg-calcite. The subsequent shallowing of the lake and increase in its salinity resulted in metamorphization of the water, an increase in the portion of $Mg^{2+}$, and precipitation of aragonite.

(4) The carbonate sediments of Lake Itkul' are significantly enriched in Sr. The study has shown that Sr is present in the sediments mostly in the carbonate form. The degree of Sr enrichment of the sediments depends on the type of carbonates. The maximum contents of Sr (an order of magnitude higher than the clarke ones) have been found in the sediment range with domination of aragonite over $CaCO_3$ and Mg-$CaCO_3$, because aragonite is much richer in Sr than calcites, especially Mg-calcite. The depth range 145–150 cm with the lowest content of calcite has the minimum content of Sr.

(5) The geochemistry of Mn in the Itkul' carbonate sediments is determined mainly by the distribution of $CaCO_3$ throughout the section: Intervals with a high content of carbonates are richer in Mn. In these highly calcareous sediments, Mn does not form its own minerals and is partly present as an isomorphic impurity in sedimentary carbonates precipitated chemically from the lake water. This is confirmed by the SEM and EPR data: The latter show that the lake carbonates contain on average 37.5% Mn and that carbonates of the aragonite-rich depth ranges of the bottom sediments are poorer in Mn.

This work was financially supported by grants 17-45-540527 and 19-05-00403 from the Russian Foundation for Basic Research, State assignment of the IGM SB RAS, and the SB RAS Integration Project "Effective use of the accelerator radiocarbon analysis in interdisciplinary research in Earth and Life sciences".

## REFERENCES

Abakumov, V.A. (Ed.), 1983. Guideline for Methods of Hydrobiological Analysis of Surface Water and Bottom Sediments [in Russian]. Gidrometeoizdat, Leningrad.

Alekin, O.A., 1970. The Fundamentals of Geochemistry [in Russian]. Gidrometeoizdat, Leningrad.

Alekin, O.A., Moricheva, N.P., 1962. Calculation of carbonate equilibrium parameters, in: Modern Methods of Natural-Water Analysis [in Russian]. Izd. AN SSSR, Moscow, pp. 158–171.

Ambatsian, P., Fernex, F., Bernat, M., Parron, C., Lecolle, J., 1997. High metal inputs to closed seas: the New Caledonian lagoon. J. Geochem. Explor. 59 (1), 59–74.

Berner, R.A., 1975. The role of magnesium in the crystal growth of calcite and aragonite from sea water. Geochim. Cosmochim. Acta 39 (4), 489–494.

Demina, L.L., Os'kina, N.S., 2012. The role of carbonate biomineralization in the geochemistry of trace elements at the early stages of oceanic sedimentation, in: The Leningrad Lithology School [in Russian]. SPbGU, St. Petersburg, Vol. 2, pp. 14–15.

Fedotov, P.S., Spivakov, B.Ya., 2008. Static and dynamic methods of fractionation of element forms in soils, muds, and bottom sediments. Uspekhi Khimii 77 (7), 690–703.

Hallam, A., Price, N.B., 1968. Further notes on the strontium contents of unaltered fossil cephalopod shells. Geol. Mag. 105 (1), 52–55.

Kennedy, W.J., Taylor, J.D., Hall, A., 1969. Environmental and biological controls on bivalve shell mineralogy. Biol. Rev. 4 (4), 499–530.

Kholodov, V.N., 2006. Geochemistry of Sedimentary Process [in Russian]. GEOS, Moscow.

Klemt, E., Kaminski, S., Miller, R., Zibold, G., Astner, M., Burger, M., Schmid, E., 2000. Normierung von Extraktionsexperimenten zur Bestimmung der Bindung von Radiocaesium an Sedimente des Luganersees, in: Umweltradioaktivität und Strahlendosen in der Schweiz. Bundesamt für Gesundheit, pp. 1–5.

Kozlovskii, E.A. (Ed.), 1984. Mining Encyclopedia [in Russian]. Sovetskaya Entsiklopediya, Moscow, Vol. 1.

Kuznetsov, A.B., 2013. Evolution of the Isotopic Composition of Strontium in the Proterozoic Ocean. ScD Thesis [in Russian].

Last, W.M., 2002. Geolimnology of salt lakes. Geosci. J. 6 (4), 347–369.

Leeder, M.R., 1982. Sedimentology: Process and Product. Springer, Dordrecht.

Li, Y.-H., 1991. Distribution patterns of the elements in the ocean: A synthesis. Geochim. Cosmochim. Acta 55, 3223–3240.

Lukashev, K.I., Kovalev, V.A., Zhukhovitskaya, A.L., Khomich, A.A., Generalova, V.A., 1971. Geochemistry of Lacustrine-Boggy Lithogenesis [in Russian]. Nauka i Tekhnika, Minsk.

Lukashin, V.N., 1981. Geochemistry of Trace Elements Involved in Sedimentation Processes in the Indian Ocean [in Russian]. Nauka, Moscow.

Mal'tsev, A.E., Leonova, G.A., Bobrov, V.A., Melenevskii, V.N., Lazareva, E.V., Krivonogov, S.K., 2014a. Diagenetic transformation of the organomineral sapropels of Lake Bol'shie Toroki (West Siberia). Geologiya i Mineral'no-Syr'evye Resursy Sibiri, No. 3, 65–76.

Mal'tsev, A.E., Leonova, G.A., Bobrov, V.A., Krivonogov, S.K., 2014b. Geochemistry of the Holocene section of the sapropel of Lake Minzelinskoe (West Siberia). Izv. Tomskogo Politekhnicheskogo Universiteta 325 (1), 83–93.

Mass Concentration of Bicarbonates and Alkalinity of Land Surface and Treated Waste Waters. Technique of Titrimetric Measurement. RD 52.24.493-2006t [in Russian], 2006. Rostov-on-Don.

Mitterer, R.M., 1972. Biogeochemistry of aragonite mud and oolites. Geochim. Cosmochim. Acta 36 (12), 1407–1422.

Monin, A.S., Lisitsyn, A.P. (Eds.), 1983. Biogeochemistry of the Ocean [in Russian]. Nauka, Moscow.

Nechiporenko, G.O., Bondarenko, G.P., 1988. Conditions of Formation of Marine Carbonates [in Russian]. Nauka, Moscow.

Organomineral Raw Materials for Agriculture of the Novosibirsk Region [in Russian], 1990. RIO PPO Pechat'. Novosibirsk.

Perel'man, A.I., 1982. Geochemistry of Natural Water [in Russian]. Nauka, Moscow.

Perel'man, A.I., 1989. Geochemistry. College Textbook [in Russian]. Vysshaya Shkola, Moscow.

Reeder, R.J., 1983. Carbonates: Mineralogy and Chemistry. Mineral. Soc. Amer., Washington.

Ricketts, R.D., Johnson, T.C., Brown, E.T., Rassmussen, K.A., Romanovsky, V.V., 2001. The Holocene paleolimnology of Lake Issyk-Kul, Kyrgyzstan: trace element and stable isotope composition of ostracodes. Palaeogeogr. Palaeoclimatol. Palaeoecol. 176, 207–227.

Schwarz, A., Turner, F., Lauterbach, S., Plessen, B., Krahn, K.J., Glodniok, S., Mischke, S., Stebich, M., Witt, R., Mingram, J., Schwalb, A., 2017. Mid- to late Holocene climate-driven regime shifts inferred from diatom, ostracod and stable isotope records from Lake Son Kol (Central Tian Shan, Kyrgyzstan). Quat. Sci. Rev. 177, 340–356.

Shotyk, W., Cheburkin, A.K., Appleby, P.G., Fankhauserd, A., Kramers, J.D., 1966. Two thousand years of atmospheric arsenic, antimony and lead deposition in an ombrotrophic bog profile, Jura Mountains, Switzerland. Earth Planet. Sci. Lett. 145, 1–7.

Shvartsev, S.L., 1998. Hydrogeochemistry of Hypergenesis Zone [in Russian]. Nedra, Moscow.

Sklyarov, E.V., Solotchina, E.P., Vologina, E.G., Ignatova, N.V., Izokh, O.P., Kulagina, N.V., Sklyarova, O.A., Solotchin, P.A., Stolpovskaya, V.N., Ukhova, N.N., Fedorovskii, V.S., Khlystov, O.M., 2010. Detailed Holocene climate record from the carbonate section of saline Lake Tsagan-Tyrm (West Baikal area). Russian Geology and Geophysics (Geologiya i Geofizika) 51 (3), 237–258 (303–328).

Solotchina, E.P., 2009. Structural Typomorphism of Clay Minerals of Sedimentary Sections and Crusts of Weathering [in Russian]. Akadem. Izd. Geo, Novosibirsk.

Solotchina, E.P., Kuzmin, M.I., Stolpovskaya, V.N., Prokopenko, A.A., Solotchin, P.A., 2008. Carbonate mineralogy of lake Hovsgol sediments: Water balance and paleoclimatic conditions. Dokl. Earth Sci. 419 (2), 438–443.

Solotchina, E.P., Sklyarov, E.V., Solotchin, P.A., Vologina, E.G., Stolpovskaya, V.N., Sklyarova, O.A., Ukhova, N.N., 2012. Reconstruction of the Holocene climate based on a carbonate sedimentary record from shallow saline Lake Verkhnee Beloe (western Transbaikalia). Russian Geology and Geophysics (Geologiya i Geofizika) 53 (12), 1351–1365 (1756–1775).

Solotchina, E.P., Solotchin, P.A., Sklyarov, E.V., 2013. Chemogenic carbonates of Holocene sediments of small salt lakes of arid zones, in: Sedimentary Basins, Sedimentation, and Postsedimentary Processes in the Geologic History. Proceedings of the Seventh All-Russian Lithological Workshop [in Russian]. Izd. SO RAN, Novosibirsk, pp. 132–136.

Syso, A.I., 2007. Regularities of the Distribution of Chemical Elements in Soil Rocks and Soils of West Siberia [in Russian]. Izd. SO RAN, Novosibirsk.

Technique of Argentometric Measurement of the Mass Concentration of Chlorides in Samples of Natural and Treated Waste Waters. PND F 14.1:2.96-97 [in Russian], 2004. Moscow.

Technique of Turbidimetric Measurement of the Mass Concentration of Sulfate Ions in Samples of Natural and Waste Waters. PND F 14.1:2.159-2000 [in Russian], 2005. Moscow.

Treshnikov, A.F., 1986. General Regularities of the Origin and Evolution of Lakes [in Russian]. Nauka, Leningrad.

Volkov, I.A., Volkova, V.S., Zadkova, I.I., 1969. Blanket Loess-like Deposits and Paleogeography of the Southwest of West Siberia in the Pliocene–Quaternary [in Russian]. Nauka, Novosibirsk.

Vorob'eva, L.A., 1998. Chemical Analysis of Soils. Textbook [in Russian]. Izd. MGU, Moscow.

Wedepohl, K.H., 1995. The composition of the continental crust. Geochim. Cosmochim. Acta 59 (7), 1217–1232.

Yudovich, Ya.E., 2007. Geochemistry of Sedimentary Rocks (Selected Chapters). Textbook [in Russian]. Syktyvkarskii Gosudarstvennyi Universitet, Syktyvkar.

Yudovich, Ya.E., Ketris, M.P., 2011. Geochemical Indicators of Lithogenesis (Lithological Geochemistry) [in Russian]. Geoprint, Syktyvkar.

Yudovich, Ya.E., Ketris, M.P., 2014. Geochemistry of Manganese [in Russian]. Geoprint, Syktyvkar.

Yudovich, Ya.E., Maidl', T.V., Ivanova, T.I., 1980. Geochemistry of Strontium in Carbonate Deposits [in Russian]. Nauka, Leningrad.

Zamana, L.V., 2009. Formation and transformation of the chemical composition of waters of mineral lakes (the example of Transbaikalia). Dokl. Earth Sci. 428 (1), 1188–1191.

Zarubina, E.Yu., 2013. Primary products of macrophytes of three sapropel lakes of different types in the south of West Siberia (within the Novosibirsk Region) in 2012. Mir Nauki, Kul'tury i Obrazovaniya, No. 5, 441–444.

*Editorial responsibility:* M.I. Kuz'min